Kirk-Othmer Encyclopedia of Chemical Technology.

DIFFUSION SEPARATION METHODS

Ordinary diffusion involves molecular mixing caused by the random motion of molecules. It is much more pronounced in gases and liquids than in solids. The effects of diffusion in fluids are also greatly affected by convection or turbulence. These phenomena are involved in mass-transfer processes, and therefore in separation processes (see Mass transfer; Separation systems synthesis). In chemical engineering, the term diffusional unit operations normally refers to the separation processes in which mass is transferred from one phase to another, often across a fluid interface, and in which diffusion is considered to be the rate-controlling mechanism. Thus, the standard unit operations such as distillation (qv), drying (qv), and the sorption processes, as well as the less conventional separation processes, are usually classified under this heading (see Absorption; Adsorption; Adsorption, gas separation; Adsorption, liquid separation).

A number of special processes have been developed for difficult separations, such as the separation of the stable isotopes of uranium and those of other elements (see Nuclear reactors; Uranium and uranium compounds). Two of these processes, gaseous diffusion and gas centrifugation, are used by several nations on a multibillion dollar scale to separate partially the uranium isotopes and to produce a much more valuable fuel for nuclear power reactors. Because separation in these special processes depends upon the different rates of diffusion of the components, the processes are often referred to collectively as diffusion separation methods. There is also a thermal diffusion process used on a modest scale for the separation of helium-group gases (qv) and on a laboratory scale for the separation of various other materials. Thermal diffusion is not discussed herein.

The most important industrial application of the diffusion separation methods has been for the enrichment of uranium-235 [5117-96-1], ^{235}U. Natural uranium consists mostly of ^{238}U and 0.711 wt % ^{235}U plus an inconsequential amount of ^{234}U. The United States was the first country to employ the gaseous diffusion process for the enrichment of ^{235}U, the fissionable natural uranium isotope. During the 1940s and 1950s, this enrichment application led to the investment of several billion dollars in process facilities. The original plants were built in 1943–1945 in Oak Ridge, Tennessee, as part of the Manhattan Project of World War II.

As of the early 1990s, diffusion separation methods are being employed or developed internationally in (*1*) Argentina, which has a gaseous diffusion project; (*2*) Brazil, where work is ongoing on gas centrifuges; (*3*) China, which has gaseous diffusion and gas centrifuges under development; (*4*) France, including Eurodif, owned by France, Italy, Spain and Belgium, which has a gaseous diffusion plant at Tricastin, plus a topping plant at Pierrelatte; (*5*) Germany, which has a large-scale centrifuge plant (Urenco); (*6*) India, which has gas centrifuges; (*7*) Japan, which has gas centrifuges; (*8*) the Netherlands, where there is a large-scale Urenco gas centrifuge plant; (*9*) Pakistan, which has gas centrifuges; (*10*) South Africa, which has a version of an advanced vortex tube process and has been working on the gas centrifuge process; (*11*) the CIS, which has large-scale gaseous diffusion and gas centrifuge plants; and (*12*) the UK, which has gaseous diffusion and Urenco gas centrifuge plants.

In the United States, a group of domestic investors, including Duke Power, and Urenco, have applied for permission to construct a new gas centrifuge plant in Louisiana.

1. General Process and Design Selection

For difficult separations, such as isotope separations that involve the separation of molecules having very similar physical and chemical properties, the enrichment that can be obtained in a single equilibrium stage or transfer unit of the process is quite small. Hence, an extremely large number of these elementary separating units must be connected to form a separation cascade in order to achieve most desired separations. Consequently, very large separation systems requiring large amounts of energy are needed, and the total energy requirement is one of the most important cost considerations.

The energy or power required by any separation process is related more or less directly to its thermodynamic classification. There are, broadly speaking, three general types of continuous separation processes: reversible, partially reversible, and irreversible.

1.1. Reversible Processes

Distillation is an example of a theoretically reversible separation process. In fractional distillation, heat is introduced at the bottom stillpot to produce the column upflow in the form of vapor which is then condensed and turned back down as liquid reflux or column downflow. This system is fed at some intermediate point, and product and waste are withdrawn at the ends. Except for losses through the column wall, etc, the heat energy spent at the bottom vaporizer can be recovered at the top condenser, but at a lower temperature. Ideally, the energy input of such a process is dependent only on the properties of feed, product, and waste. Among the diffusion separation methods discussed herein, the centrifuge process (pressure diffusion) constitutes a theoretically reversible separation process.

1.2. Partially Reversible Processes

In a partially reversible type of process, exemplified by chemical exchange, the reflux system is generally derived from a chemical process and involves the consumption of chemicals needed to transfer the components from the upflow into the downflow at the top of the cascade, and to accomplish the reverse at the bottom. Therefore, although the separation process itself may be reversible, the entire process is not, if the reflux is not accomplished reversibly.

Insofar as the consumption of chemicals is concerned, it is obvious that the total consumption of reflux-producing chemicals is proportional to the interstage flows, or width of the cascade, but independent of the number of stages in series, or length of the system.

1.3. Irreversible Processes

Irreversible processes are among the most expensive continuous processes. These are used only in special situations, such as when the separation factors of more efficient processes (that is, processes that are theoretically more efficient from an energy point of view) are found to be uneconomically small. Except for pressure diffusion, the diffusion methods discussed herein are essentially irreversible processes. Thus, gaseous diffusion, in which gas expands from a region of high pressure to one of low pressure, mass diffusion, in which a vapor flows from a region of high partial pressure to one of low partial pressure, and thermal diffusion, in which heat flows from a high temperature source to a low temperature sink, are all irreversible processes. In contrast with reversible and partially reversible processes, the energy demand in an irreversible process is distributed over the whole cascade in direct proportion to the distribution flow.

In gaseous diffusion, the cascade consists of individual stages that are connected in series. In each stage part of the gaseous feed is forced through a diffusion membrane or barrier with holes smaller than the mean free path of the gas (see Membrane technology). Because of slightly greater mobility, the lighter components

flow preferentially through the barrier. This enriched portion of the feed is transported to a neighboring stage, up the cascade, where the lighter components tend to concentrate. The other portion of the gas that does not pass through the barrier is rejected to a neighboring stage, down the cascade, where the heavier components tend to concentrate. The feed to each stage is thus composed of combined upflow and downflow from neighboring stages.

In pressure diffusion, a pressure gradient is established by gravity or in a centrifugal field. The lighter components tend to concentrate in the low pressure (center) portion of the fluid. Countercurrent flow and cascading extend the separation effect.

Irreversible processes are mainly applied for the separation of heavy stable isotopes, where the separation factors of the more reversible methods, eg, distillation, absorption, or chemical exchange, are so low that the diffusion separation methods become economically more attractive. Although application of these processes is presented in terms of isotope separation, the results are equally valid for the description of separation processes for any ideal mixture of very similar constituents such as close-cut petroleum fractions, members of a homologous series of organic compounds, isomeric chemical compounds, or biological materials.

2. Cascade Design

Less conventional diffusional separation operations are characterized by the relatively small separations that can be obtained by the elementary separation mechanism. That is, the changes in fluid composition attained in gaseous diffusion across the barrier, in thermal diffusion between the hot and cold walls, in mass diffusion between the inlet and the condensing surface for the sweep vapor, and in the centrifuge between the axis of the rotor and its periphery, are all quite small. Thus, a large number of separating units must be employed. *Cascade* is the term given to the aggregation of separating units that have been interconnected so as to be able to produce the desired material. The optimum arrangement of the separating units in a separation cascade generally minimizes the unit cost of product, and its design is a problem common to all separation processes. In a stagewise separation process such as gaseous diffusion, each unit of equipment consists of one separation stage.

2.1. The Separation Stage

A fundamental quantity, α, exists in all stochastic separation processes, and is an index of the steady-state separation that can be attained in an element of the process equipment. The numerical value of α is developed for each process under consideration in the subsequent sections. The separation stage, which in a continuous separation process is called the transfer unit or equivalent theoretical plate, may be considered as a device separating a feed stream, or streams, into two product streams, often called heads and tails, or product and waste, such that the concentrations of the components in the two effluent streams are related by the quantity, α. For the case of the separation of a binary mixture this relationship is

$$\left(\frac{y}{1-y}\right) \Big/ \left(\frac{x}{1-x}\right) = \alpha \qquad (1)$$

where y is the mol fraction of the desired component in the upflowing (heads) stream from the stage and x the mol fraction of the same component in the down-flowing (tails) stream from the stage. The quantity α is usually called the stage separation factor.

For the case of separating a binary mixture, the following conventions are used. The concentrations of the streams are specified by the mol fraction of the desired component. The purpose of the separation process

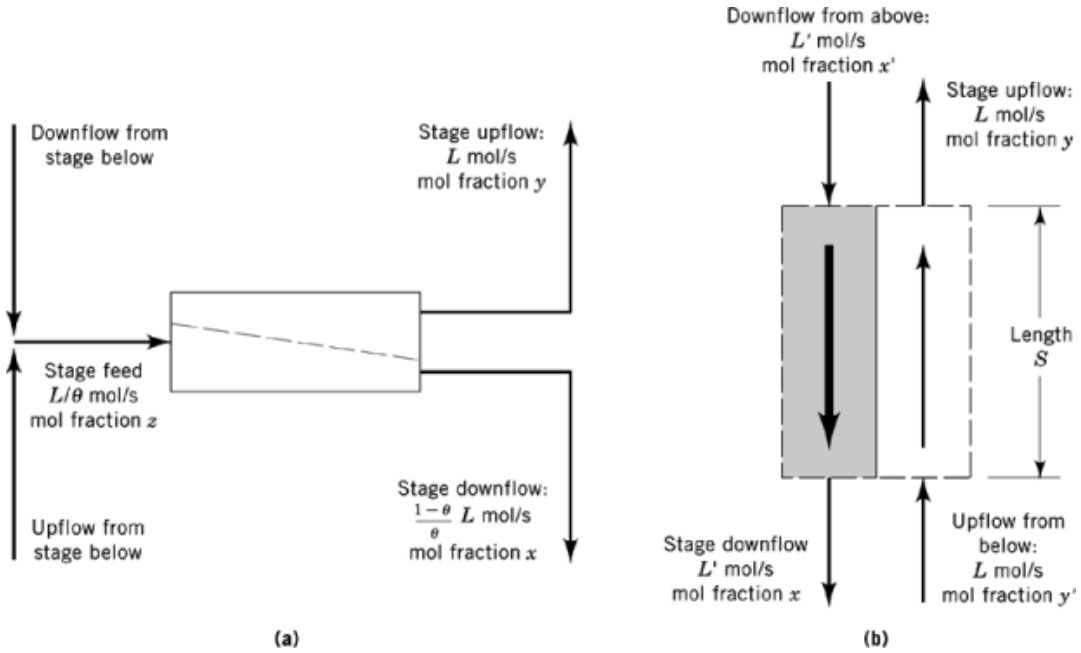

Fig. 1. The analogy between the separation stage and the transfer unit or equivalent theoretical plate: (**a**) in a stagewise process; (**b**) in a continuous-separation process. The terms are defined in text.

is usually to obtain one component of the mixture in an enriched form. If both components are desired, the choice of the desired component is an arbitrary one. The upflowing stream from the separation stage is the one in which the desired component is enriched, and by virtue of this convention, α is defined as a quantity the value of which is greater than unity. However, for the processes considered here, α exceeds unity by only a very small fraction, and the relationship between the concentrations leaving the stage can be written, without appreciable error, in the form

$$y - x = (\alpha - 1)\, x\, (1 - x) \qquad (2)$$

A separation stage or transfer unit operating on a binary mixture is shown schematically in Figure 1. In a cascade of separating stages, the feed stream can be formed by mixing the downflowing stream from the stage above and the upflowing stream from the stage below. The quantity, θ, ie, the fraction of the combined stage feed that goes into the stage upflow stream, is termed the cut of the stage. In cascades ordinarily designed for difficult separations, the stage cut is normally very nearly equal to one-half. In the case of a theoretical plate in a continuous process, the feed consists of two separate streams, one from above and one from below. In cascades for either stagewise or continuous processes the upflow rate L and the downflow rate L' (or $L(1-\theta)/\theta$) are very nearly equal. For continuous process units, the length S is the length of equipment necessary to satisfy the requirement of equation 1, that the streams leaving the unit be related by α; it is usually called the height of a transfer unit (HTU) or the height equivalent to a theoretical plate (HETP). Although the HTU and HETP are defined differently and are not precisely equivalent to each other, the difference between them becomes negligible when the value of the quantity $\alpha - 1$ is small.

2.2. The Separative Capacity

The separation stage is characterized not only by the separation factor α but also by its capacity or throughput of which the upflow L is a measure, and in the case of the continuous process, also by the length S. It is therefore desirable to define and determine a quantity indicative of the amount of useful separative work that can be done per unit time by a single stage. Such a quantity is called the separative capacity of the stage. It is postulated that the separation stage does useful work on the streams it processes, hence increasing their net value. The value of a stream must be a function of its concentration; let this value function be designated by $v(x)$. Then the separative capacity of the stage by definition is set equal to the increase in value it creates. The separative capacity of a unit is a very useful concept and permits comparisons to be made between different separation processes.

The separative capacity of the stage, termed δU, is set equal to the net increase in value of the streams it processes (see Fig. 1):

$$\delta U = Lv(y) + \frac{1-\theta}{\theta} Lv(x) - \frac{1}{\theta} Lv(z) \qquad (3)$$

The value functions appearing in equation 3 may be expanded in Taylor series about x and, because the concentration changes effected by a single stage are relatively small, only the first nonvanishing term is retained. When the value of z is replaced by its material balance equivalent, ie, equation 4:

$$z = (1-\theta)x + \theta y \qquad (4)$$

the separative capacity of the stage is given by:

$$\delta U = \frac{1}{2} L(1-\theta)\ (y-x)^2 v''(x) \qquad (5)$$

where $v''(x)$ is the second derivative of the value function. The concentrations y and x are related by equation 2; thus the separative capacity can also be written as:

$$\delta U = \frac{1}{2} L(1-\theta)\ (\alpha-1)^2 x^2 (1-x)^2 v''(x) \qquad (6)$$

As it is desirable that the separative capacity of the stage be independent of the concentration of the material with which it is operating, the terms in the equation involving the concentration are set equal to a constant, taken for convenience to be unity, and the separative capacity of a single stage operating with a cut of one-half is seen to be:

$$\delta U = \frac{1}{4} L(\alpha-1)^2 \qquad (7)$$

Thus, the separative capacity of a stage is directly proportional to the stage upflow as well as to the square of the separation effected.

2.2.1. Equivalent Theoretical Plate

The separative capacity of a theoretical plate in a continuous process can be obtained in the same manner. By equating the separative capacity of the unit to the net increase in value of the four streams handled (eq. 8):

$$\delta U = Lv(y) + L'v(x) - Lv\left(y'\right) - L'v\left(x'\right) \qquad (8)$$

After expansion in Taylor series about the concentration x and replacing the concentration y' by its material balance equivalent:

$$\delta U = L\left(y - x'\right)\ \left(x' - x\right) v''(x) \qquad (9)$$

The separative capacity of the equivalent theoretical stage in the continuous process is seen to depend on the concentration difference between the countercurrent streams as well as on the concentration difference between the top and bottom of the stage. The separative capacity is zero when x' is equal to y or x' is equal to x; inspection shows that it attains a maximum value when x' is equal to the arithmetic average of x and y and that this maximum value is:

$$(\delta U)_{\max} = \frac{1}{4} L(y - x)^2 v''(x) = \frac{1}{4} L(\alpha - 1)^2 \qquad (10)$$

Thus, the maximum value of the separative capacity of a theoretical plate in a continuous process is equal to that of a single separation stage when both units have the same value of the $L(\alpha - 1)^2$ product. When the continuous process is operated so as to yield its maximum separative capacity, the concentrations y' and x' of the streams entering the unit are equal and the similarity between the separation stage and the theoretical plate is accentuated because, for this case, both may be considered to separate a single feed stream into two product streams having concentrations related by α. The definition of a theoretical plate in the continuous process is essentially arbitrary and not required; however, it is a useful concept, permitting both the stagewise and continuous processes to be treated with the same set of cascade equations.

2.2.2. The Value Function

The value function itself is defined, as has been indicated above, by the second-order differential:

$$v''(x) = 1/\left[x^2 (1 - x)^2\right] \qquad (11)$$

In the design of cascades, a tabulation of $v(x)$ and of $v'(x)$ is useful. The solution of the above differential equation contains two arbitrary constants. A simple form of this solution results when the constants are evaluated from the boundary conditions $v(0.5) = v'(0.5) = 0$. The expression for the value function is then:

$$v(x) = (2x - 1) \ln\left[x/(1 - x)\right] \qquad (12)$$

and for the derivative of the value function (eq. 13):

$$v'(x) = \frac{2x - 1}{x(1 - x)} + 2\ln\frac{x}{1 - x} \qquad (13)$$

Therefore, $v(1 - x) = v(x)$ and $v'(1 - x) = -v'(x)$.

2.2.3. Application

In addition to providing a relatively simple means for estimating the production of separation cascades, the separative capacity is useful for solving some basic cascade design problems; for example, the problem of determining the optimum size of the stripping section.

It can be assumed that P, y_P, and x_F for the cascade have been specified, and that the cost of feed and the cost per unit of separative work, the product of separative capacity and time, are known. The basic assumption

is that the unit cost of separative work remains essentially constant for small changes in the total plant size. The cost of the operation can then be expressed as the sum of the feed cost and cost of separative work:

$$C_{\text{total}} = (C_F)\ (F)\ (\Delta t) + C_{\Delta U}\,[Pv\,(y_P) + Wv\,(x_W) - Fv\,(x_F)]\,\Delta t \qquad (14)$$

where C_{total} is the total cost of operation for the period of time Δt, and C_{F} and $C_{\Delta U}$ are the cost per unit of feed and the cost per unit of separative work, respectively. The optimum value of x_{W} is that which minimizes the total cost and can be found by differentiating the total cost with respect to x_{W} under the restrictions that P, y_{P}, and x_{F} remain constant, and setting the result equal to zero. The result of this procedure is that the optimum x_{W} is the solution to equation 15:

$$v\,(x_F) - v\,(x_W) - (x_F - x_W)\,v'\,(x_W) = C_F/C_{\Delta U} \qquad (15)$$

When the cascade is operated using the optimum x_{W}, the cost of producing material at any other concentration, y_{P}, is given by:

$$C_{\text{total}} = C_{\Delta U} P\left[v\,(y_P) - v\,(x_W) - (y_P - x_w)\,v'\,(x_W)\right]\Delta t \qquad (16)$$

obtained by combining equations 14 and 15. An equation of this form can be used to establish the value of material of different concentrations from separation cascades.

2.3. Cascade Gradient Equations

An arrangement of separation stages to form a simple cascade is shown in Figure 2. A simple cascade is one that divides a single cascade feed stream into a product stream and a waste stream. Additional side streams, however, could easily be handled. To be consistent with the conventions given for the single stage, the desired component is assumed to be enriched in the product stream at the top of the cascade. The cascade feed is introduced at some intermediate stage between the top and bottom of the cascade. The portion of the cascade that lies above the feed point is termed the enriching section; that which lies below the feed point is termed the stripping section. The gradient equations for the cascade are obtained from a combination of the material balance equations, frequently called the operating-line equations, and the α relationship, usually called the equilibrium-line equation. From a material balance around the top of the cascade down to, but not including, stage n of the enriching section, is obtained the operating-line equation:

$$L_n y_n = (L_n - P)\,x_{n+1} - P y_P \qquad (17)$$

which can be combined with the equilibrium-line (eq. 2) to give:

$$x_{n+1} - x_n = \frac{L_n}{L_n - P}\left[(\alpha - 1)\,x_n\,(1 - x_n) - (P/L_n)\ (y_P - x_n)\right] \qquad (18)$$

For the case under consideration, where the value of $\alpha - 1$ is quite small, it follows that everywhere in the cascade, except possibly at the extreme ends, the stage upflow is many times greater than the product withdrawal rate. Thus $L/(L - P)$ can be set equal to unity. Furthermore when the value of $\alpha - 1$ is small, the stage enrichment $x_{n+1} - x_n$ can be approximated by the differential ratio dx/dn without appreciable error. The gradient equation for the enriching section of a simple cascade therefore takes the form

$$dx/dn = (\alpha - 1)\,x\,(1 - x) - (P/L)\ (y_P - x) \qquad (19)$$

Similarly, one obtains a gradient equation for the stripping section that has the form

$$dx/dn = (\alpha - 1)\,x\,(1 - x) - (W/L)\;(x - x_W) \qquad (20)$$

Equations 19 and 20 are the basic equations for cascade design. Although these equations were derived from a consideration of a cascade composed of discrete separation stages, equations of the same form are also obtained for cascade designs based on continuous or differential separation processes. For use in the case of continuous separation processes, however, the term dx/dn, which is the enrichment per stage, is usually replaced by the equivalent terms $S\,dx/dz$, where S is the stage length and dx/dz the enrichment per unit length of process equipment. These equations may then be used to calculate the output from a given cascade configuration, that is, from a cascade for which the variation of $\alpha - 1$ and L is known as a function of the stage number.

2.3.1. Minimum Length or Minimum Number of Stages

It is evident from the gradient equations that the enrichment per stage decreases as the withdrawal rate increases. Thus the minimum number of stages required to span a given concentration difference is obtained when no material is withdrawn from the cascade. This mode of operation ($P = W = F = 0$) is frequently called total reflux operation. Integration of the gradient equation for this case with $\alpha - 1$ taken to be constant gives:

$$N_{\min} = \frac{1}{\alpha - 1} \ln \left(\frac{x_T}{1 - x_T} \Big/ \frac{x_B}{1 - x_B} \right) \qquad (21)$$

where the concentration range to be spanned is from the concentration x_B at the bottom to concentration x_T at the top. As an example of the magnitudes involved, consider the enrichment of ^{235}U by gaseous diffusion from $x_B = 0.005$ to $x_T = 0.90$. For a value of α equal to 1.0043 the minimum number of diffusion stages required is 1742.

2.3.2. Minimum Width or Minimum Stage Upflow

It also follows directly from the gradient equations that if the withdrawal rates from the cascade are nonzero, it is necessary that the stage upflow from the stage at which the cascade concentration is x must exceed some critical value in order that there be any enrichment at that point in the cascade. This critical value is called the minimum stage upflow and is obtained by setting dx/dn equal to zero in the gradient equation. Thus, for any point in the enriching section the minimum stage upflow is given by

$$L_{\min} = P\,(y_P - x) / \left[(\alpha - 1)\,x\,(1 - x)\right] \qquad (22)$$

For the case of enriching ^{235}U to 90 mol % product concentration, the stage upflow at the feed point ($x_F = 0.0072$) must therefore exceed 29,046 times the product withdrawal rate. It can now be seen from a consideration of the minimum stage upflow that the approximation made in deriving the gradient equation, ie, taking the quantity $(1 - P/L)$ equal to unity, introduces negligible error except possibly in the immediate vicinity of the withdrawal points. The condition that arises in a cascade at points where the stage upflow approaches the value $L_{\min}$ is commonly called pinching.

2.3.3. Gradient Equations for a Square Section

A section of a cascade composed of identical stages, that is, a number of stages having the same separation factor and the same stage upflow, is called a square section. For sections of this type the gradient equations are readily integrable. For a section in the enricher of a cascade producing material at rate P and concentration

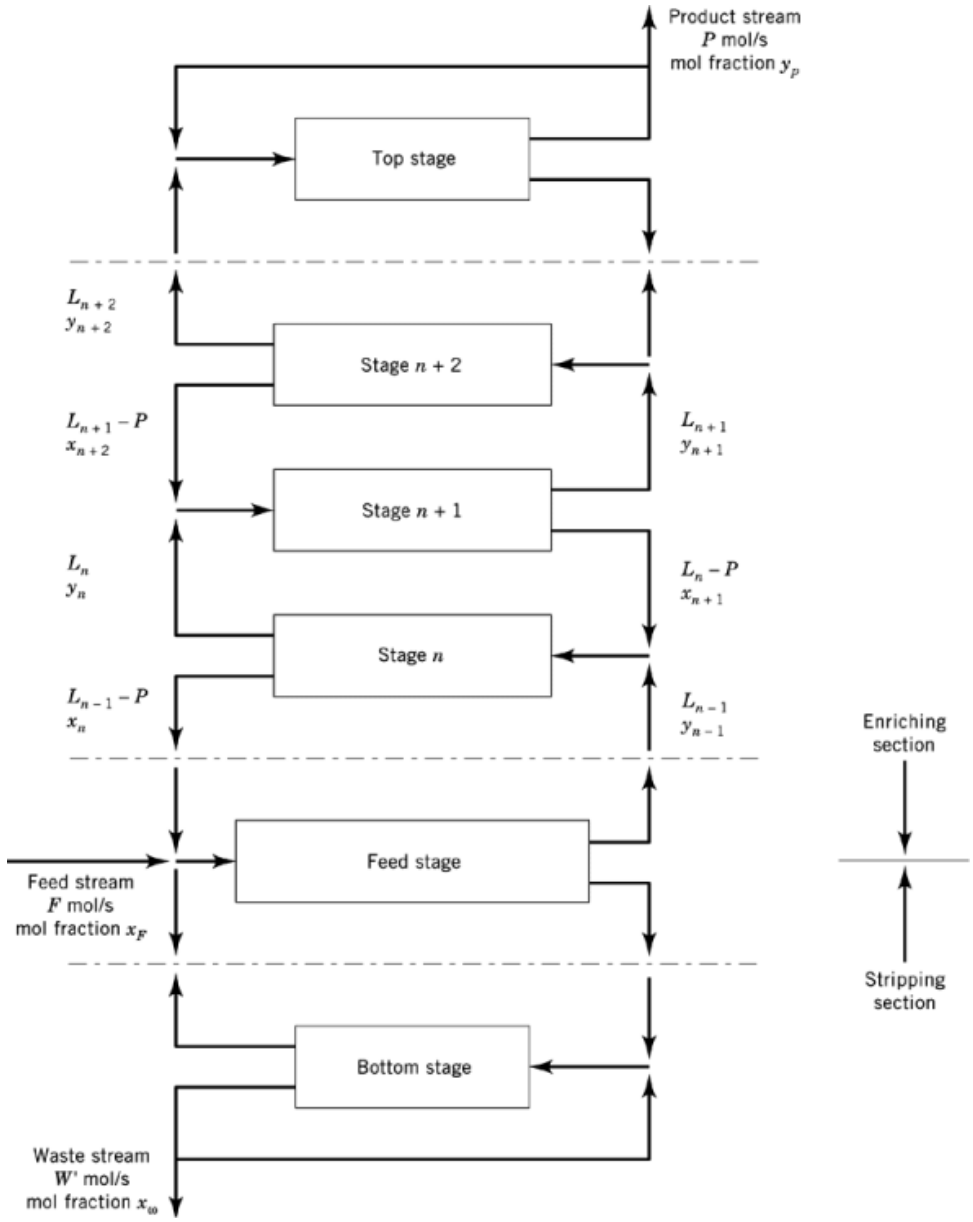

Fig. 2. Separation stages arranged to form a simple cascade. Terms are defined in text.

y_P, the solution can be written:

$$N_{\text{sect}} = \left[(\alpha - 1)\ (X_1 - X_0)\right]^{-1} \ln \frac{(X_1 - x_B)\ (x_T - X_0)}{(X_1 - x_T)\ (x_B - X_0)} \qquad (23)$$

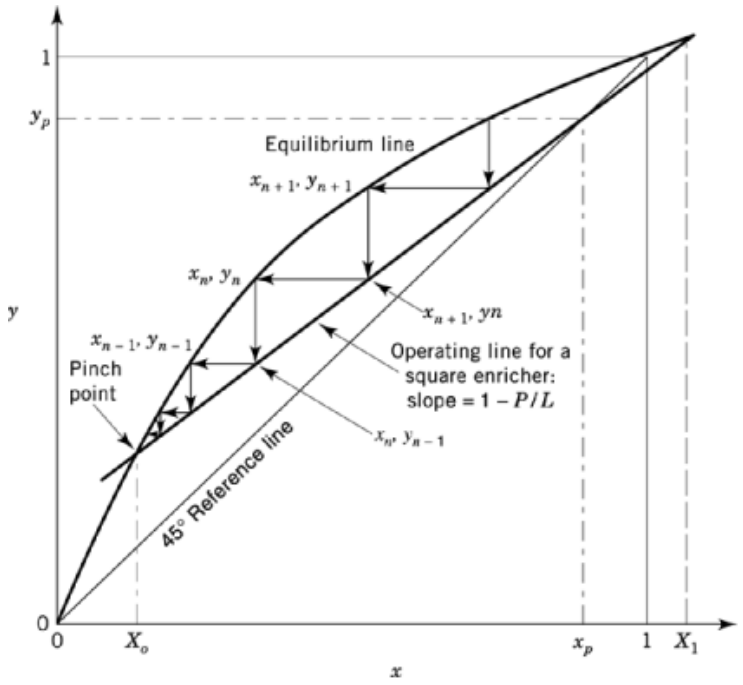

Fig. 3. A McCabe-Thiele diagram for a hypothetical square cascade section illustrating pinching. Terms are defined in text.

where X_1 and X_0 are the roots of a quadratic equation and are given by:

$$X_1, X_0 = \frac{L(\alpha - 1) + P \pm \{[L(\alpha - 1) + P]^2 - 4L(\alpha - 1)Py_P\}^{1/2}}{[2L(\alpha - 1)]} \qquad (24)$$

and N_{sect} is the number of stages necessary to span the concentration difference from x_{B} at the bottom of the section to x_{T} at the top of the section. Equation 23 is also obtained for a square section in the stripping section, but in the case of the stripper the value of X_1 and X_0 are given by:

$$X_1, X_0 = \frac{\{L(\alpha - 1) - W \pm \{[L(\alpha - 1) - W]^2 + 4L(\alpha - 1)Wx_W\}^{1/2}\}}{[2L(\alpha - 1)]} \qquad (25)$$

2.3.4. Graphical Solution

Some of the preceding concepts can be illustrated graphically by means of a McCabe-Thiele diagram, shown in Figure 3. In such a diagram the equilibrium line, equations 1 or 2, and the operating line, equation 17, are plotted on a set of *x, y* coordinates. For the case of a square cascade section, the operating line is straight and has the slope $(1 - P/L)$: if the section lies at the product withdrawal end of the cascade, its opening line passes through the point $x = y = y_P$, as shown. The number of stages required to span a given concentration difference, or conversely the concentration difference obtained across a square section with a given number of stages can be illustrated in such a figure.

It is evident from the construction that the closer the operating line lies to the 45-degree reference line, the fewer the number of stages required to span a given concentration difference. The minimum number of stages is therefore required when the operating line coincides with the 45-degree line, that is, when P/L is equal to zero. It is also evident that in the neighborhood of a point of intersection of the operating and equilibrium lines the enrichment per stage becomes quite small and is equal to zero at the point of intersection itself. At such a point pinching is said to occur, and the origin of the term is made clear by the diagram. In order for a cascade section to span a concentration difference from x_B to y_P, it follows that the operating line may not intersect the equilibrium line before the concentration x_B is reached; the value of L for which the two curves intersect at x_B is the minimum upflow corresponding to the cascade concentration x_B. It is also noteworthy that the values X_0 and X_1 appearing in equations 23 through 25 are the x coordinates of the two points of intersection of the operating line of a square section with the equilibrium line. Although the graphical solution of the cascade gradient equation is simple in principle and exact in theory, it becomes quite cumbersome in practice when processes having separation factors close to unity and hence cascades with thousands of stages are under consideration. For this reason analytic solutions to the gradient equation are usually preferred.

2.4. The Ideal Cascade

A cascade of particular interest to design engineers is the ideal cascade: a continuously tapered cascade (ie, L is a continuously varying function of x or n) that has the property of minimizing the sum of the stage upflows of all the stages required to achieve a given separation task. Because, in general, the total volume of the equipment required and the total power requirement of the cascade are directly proportional to the sum of the stage upflows, a consideration of the ideal plant requirements often permits a good economic estimate of the unit cost of product to be made without having to resort to the much more painstaking labor of designing a real (as opposed to ideal) cascade to accomplish the separation job. A simple, intuitive approach to the ideal cascade concept in the case of a cascade composed of discrete stages follows. Again, the resulting equations are also valid for a cascade based on a continuous or differential separation process.

For the case of a stagewise enrichment process the ideal cascade may be defined as one in which there is no mixing of streams of unequal concentrations. Clearly, the mixing of streams of unequal concentrations in the cascade to form the feed to a separation stage constitutes an inefficiency because it is precisely the reverse of the process taking place in the stage itself. Figure 2 shows that the no-mixing condition at the entrance to stage $n+1$ requires that $y_n = x_{n+2}$. If the enrichment per stage is essentially constant, $x_n + 2$ may be written as $x_n + 2(dx/dn)$. The concentration y_n is related to x_n by the α-relationship (eq. 2). Thus the no-mixing condition leads directly to the gradient equation for the ideal plant:

$$\frac{dx}{dn} = \frac{\alpha - 1}{2} x(1 - x) \qquad (26)$$

The number of stages required to span a given concentration difference in an ideal plant in which all stages have the same separation factor is therefore

$$N_{\text{ideal}} = \frac{2}{\alpha - 1} \ln \left(\frac{x_T}{1 - x_T} \Big/ \frac{x_R}{1 - x_R} \right) = 2N_{\min} \qquad (27)$$

and is twice the minimum number of stages required. The combination of equations 19 and 26 gives the equation for the stage upflow at any point in the enricher of an ideal cascade that is twice the minimum upflow

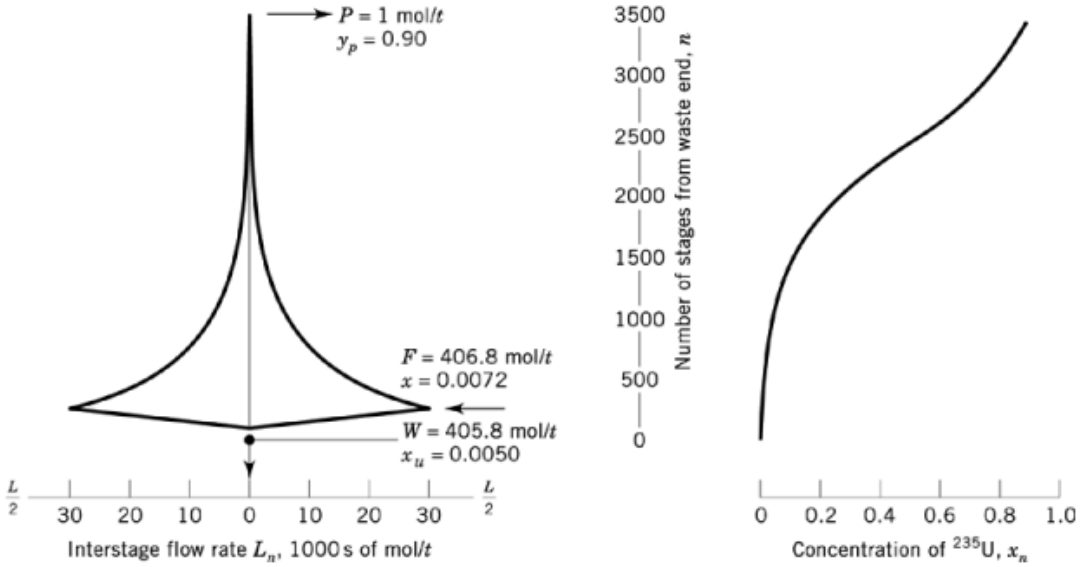

Fig. 4. Characteristics of an ideal separation cascade for uranium isotope separations. For this cascade: $_{\alpha}$=1.0043; N_T=3484 stages; $_{\Delta}U$=153.08mol/t; ΣL_T=33.116×102 mol/t, where t represents unit time.

$$L_{\text{ideal}} = \frac{2P(y_P - x)}{(\alpha - 1)x(1 - x)} = 2L_{\min} \qquad (28)$$

Equations 27 and 28 can be used in conjunction, along with the corresponding equations for the stripping section, to produce an ideal plant profile such as is shown in Figure 4 where L_{ideal} is plotted against N_{ideal} for the example of an ideal cascade to produce one mol of uranium per unit time enriched to 90 mol % in ^{235}U from natural feed containing 0.72 mol % ^{235}U, with a waste stream rejected at a concentration of 0.5% ^{235}U. The characteristic lozenge shape of the ideal cascade is evident: no two stages in either the enricher or stripper are the same size. It can be deduced from the above statements that, except at the terminals, the operating line for an ideal cascade on a McCabe-Thiele diagram is a curved line lying midway between the equilibrium line and the 45° reference line.

2.4.1. Total Upflow in an Ideal Plant

The sum of the upflows from all of the stages in the ideal plant, or more simply, the total upflow, is the area enclosed by the cascade shown in Figure 4. An analytical expression for this quantity is obtained as the summation of all the stage upflows in the enriching section expressed as an integral:

$$\sum^{\text{enr}} L_n = \int L dn = \int_{x_F}^{y_P} L \frac{dn}{dx} dx \qquad (29)$$

For the ideal cascade, L is given by equation 28 and dx/dn by equation 26. Making these substitutions:

$$\sum^{\text{enr}} L_n = \int_{x_F}^{y_P} \frac{4P}{(\alpha-1)^2} \frac{(y_P - x)}{x^2(1-x)^2}\, dx \qquad (30)$$

However, recalling the definition of the value function, equation 11, and assuming that the value of α is the same for all stages, the integral may be written in the form:

$$\sum^{\text{enr}} L_n = \frac{4P}{(\alpha-1)^2} \int_{x_F}^{y_P} (y_P - x)\, v''(x)\, dx \qquad (31)$$

which is readily integrated by parts to give:

$$(\text{total upflow})_{\text{enr}} = \left[4P/(\alpha-1)^2\right] \left[v(y_P) - v(x_F) - (y_P - x_F)\, v'(x_F)\right] \qquad (32)$$

The equation for the total flow in the stripping section is obtained in the same manner:

$$(\text{total upflow})_{\text{str}} = \left[4W/(\alpha-1)^2\right] \left[v(x_W) - v(x_F) - (x_W - x_F)\, v'(x_F)\right] \qquad (33)$$

The total flow in the cascade is then given by the sum of equations 32 and 33, which can be simplified with the use of the cascade material balances:

$$P + W = F \qquad (34)$$

and

$$Py_P + Wx_W = Fx_F \qquad (35)$$

to give the convenient form

$$(\text{total upflow})_{\text{cascade}} = \left[4/(\alpha-1)^2\right] \left[Pv(y_P) + Wv(x_W) - Fv(x_F)\right] \qquad (36)$$

For the example considered above, the total cascade upflow is found to be 33×10^6 mols per unit time.

The second term in brackets in equation 36 is the separative work produced per unit time, called the separative capacity of the cascade. It is a function only of the rates and concentrations of the separation task being performed, and its value can be calculated quite easily from a value balance about the cascade. The separative capacity, sometimes called the separative power, is a defined mathematical quantity. Its usefulness arises from the fact that it is directly proportional to the total flow in the cascade and, therefore, directly proportional to the amount of equipment required for the cascade, the power requirement of the cascade, and the cost of the cascade. The separative capacity can be calculated using either molar flows and mol fractions or mass flows and weight fractions. The common unit for measuring separative work is the separative work unit (SWU) which is obtained when the flows are measured in kilograms of uranium and the concentrations in weight fractions.

The great utility of the separative capacity concept lies in the fact that if the separative capacity of a single separation element can be determined, perhaps from equations 7 or 10, then the total number of such identical elements required in an ideal cascade to perform a desired separation job is simply the ratio of the

separative capacity of the cascade to that of the element. The concept of an ideal plant is useful because moderate departures from ideality do not appreciably affect the results. For example, if the upflow in a cascade is everywhere a factor of m times the ideal upflow, the actual total upflow required to perform a separative task is $m^2/(2m-1)$ times the ideal cascade total upflow. Thus, if the upflow is 20% greater than ideal at every point in that cascade ($m = 1.2$), the number of separation elements would be only 2.86% greater than that calculated from ideal cascade considerations.

2.5. Equations for Large Stage Separation Factors

The preceding results have been obtained with the use of equation 2 and by replacing the finite difference, $x_{n+1} - x_n$, by the differential, dx/dn, both of which are valid only when the quantity $(\alpha - 1)$ is very small compared with unity. However, there has been renewed interest, partly because of the development of the gas centrifuge process to commercial status, in the design of cascades composed of stages with large stage separation factors. When the stage separation factor is large, the number of stages required in an ideal cascade in which all stages have the same separation factor is given by

$$N_{\text{ideal}} = \frac{2}{\ln\alpha} \ln\left(\frac{y_P}{1-y_P} \Big/ \frac{x_W}{1-x_W} \right) - 1 \qquad (37)$$

instead of equation 27. When dealing with cascades composed of stages having large separation factors, it is somewhat more convenient to calculate the sum of all the stage feed flows in the cascade rather than the sum of all the stage upflows as was done in the case when $(\alpha - 1)$ is small. When $(\alpha - 1)$ is small with respect to unity, the stage feed flow is essentially just twice the stage upflow rate, and the stage feed flow rate in an ideal cascade (see eq. 28) is:

$$(L/\theta)_{\text{ideal}} = \frac{4P(y_P - x)}{(\alpha - 1)x(1-x)} \qquad (38)$$

However, when α is large, the corresponding equation for the stage feed rate takes the form

$$(L/\theta)_{\text{ideal}} = \frac{(\alpha)^{1/2} + 1 P(x_P - z)}{(\alpha)^{1/2} - 1 z(1-z)} \qquad (39)$$

The sum of the stage feed flow rates of all of the stages in an ideal cascade is just twice the total cascade upflow rate when $(\alpha - 1)$ is small with respect to unity, or

$$(\text{total stage feed})_{\text{cascade}} = \frac{8}{(\alpha-1)^2} \left[P v(y_P) + W v(x_W) - F_V(x_F) \right] \qquad (40)$$

but is given by

$$(\text{total stage feed})_{\text{cascade}} = \frac{2}{\ln\alpha} \frac{(\alpha)^{1/2} + 1}{(\alpha)^{1/2} - 1} \left[P v(y_P) + WV(x_W) - FV(x_F) \right] \qquad (41)$$

when α is larger. It can be seen that when α is close to unity, equation 41 gives the same result as equation 40. However, if α is equal to 1.1, the total stage feed would be underestimated by 9.2%, and if α is equal to 2.0, the total stage feed would be underestimated by 42.4%, using equation 40 instead of equation 41. Some of the work in this area of cascade theory has dealt with the design of cascades using asymmetric isotope separation

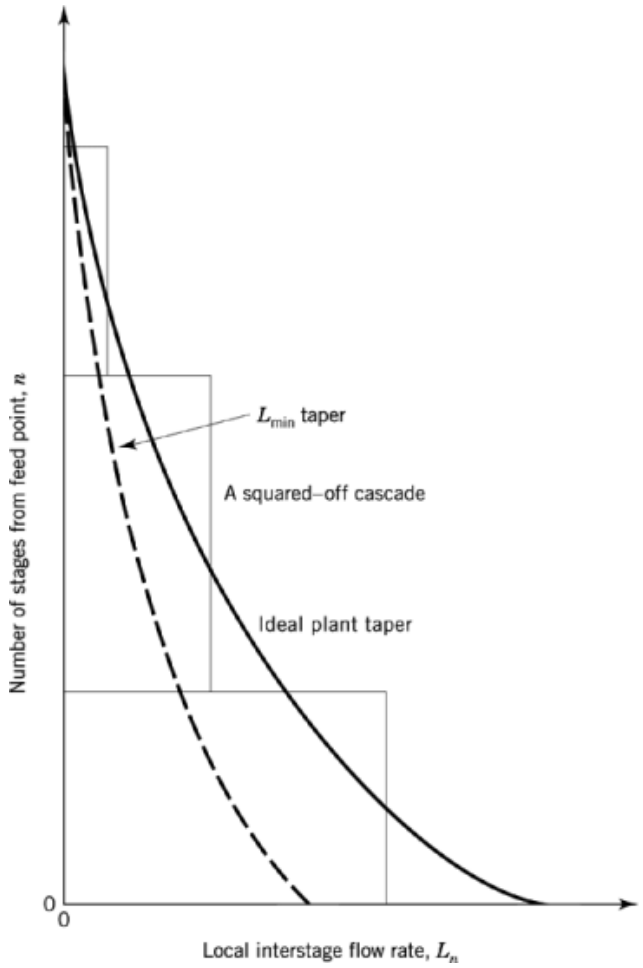

Fig. 5. Design of a real cascade obtained by squaring off an ideal enriching section.

stages (1, 2) with the analysis of two-up, one-down cascades, that is, cascades in which the upflow from the n^{th} stage in the cascade bypasses the $(n+1)^{\text{th}}$ stage and is reintroduced at the $(n+2)^{\text{th}}$ stage.

2.6. Real Cascades

Although the ideal cascade minimizes the volume of equipment and the energy requirements, the cost of the cascade is generally not minimized because production economies are realized in the manufacture of the process equipment when a large number of identical units are produced. Thus, a minimum-cost cascade consists of a number of square cascade sections rather than uniformly tapered nonidentical stages. A first approximation to the optimum practical cascade, once the size (length and width) of the individual separating units available is known, is obtained by fitting the ideal plant shape with square sections in some intuitively appealing manner, as illustrated in Figure 5.

Figure 5 shows an ideally tapered enricher that has been replaced by three square cascade sections, a process called squaring-off the cascade (3–6). During the squaring-off process, two essential requirements must

be kept in mind: The interstage flow in all-square sections must always exceed the local value of $L_{\min}$ at all points in the cascade, and the squared-off cascade must contain a total number of stages which exceeds $N_{\min}$. In order for the squared-off cascade to give a performance closely resembling that of the ideal cascade, the shape of the squared-off cascade should approximate the shape of the ideal cascade.

In the final analysis the problem of determining the optimum practical cascade is rather complex. Equipment performance and costs need to be related to the selected independent process variables. The main process equipment usually consists of a large number of separating units, pumping and heat exchange equipment, control devices, and connecting piping. The whole process is provided with services, and auxiliary systems and feed and withdrawal facilities. It is usually enclosed by a building and surrounded by land of the proper type. Sizes and cost of these important items must be related to the process variables. The details of procedures used for the optimization of real gaseous diffusion cascades are presented in Reference 7, and the problems of optimization of real gas centrifuge cascades are discussed in Reference 8.

2.7. Time-Dependent Cascade Behavior

The period of time during which a cascade must be operated from start-up until the desired product material can be withdrawn is called the *equilibrium time* of the cascade. The equilibrium time of cascades utilizing processes having small values of $\alpha - 1$ is a very important quantity. Often a cascade may prove to be quite impractical because of an excessively long equilibrium time. An estimate of the equilibrium time of a cascade can be obtained from the ratio of the enriched inventory of desired component at steady state, H, to the average net upward transport of desired component over the entire transient period from start-up to steady state, $\overline{\tau}$;. In equation form this definition can be written as

$$T_{\text{eq}} = H/\bar{\tau} = \frac{1}{\bar{\tau}} \int_0^N h_n (x_n - x_F)\, dn \qquad (42)$$

where h_{n} is the holdup of the n^{th} stage. The average net upward transport for the entire transient period is not usually known; the initial and final values of the net transport, however, are known. At start-up the concentration gradient is flat, because the column is filled with material at feed concentration, and the transport is a maximum. Using this transport in equation 42 gives a lower limit for the equilibrium time

$$\left(T_{\text{eq}}\right)_{\min} = H/\left[L(\alpha - 1)\, x_F (1 - x_F)\right] \qquad (43)$$

At steady state, with a fully developed gradient, the net transport is $P(y_P - x_F)$, which is a lower limit for net upward transport. Substituting this into equation 42, leads to an expression for an upper limit for the equilibrium time:

$$\left(T_{\text{eq}}\right)_{\max} = H/\left[P(y_P - X_F)\right] \qquad (44)$$

Equations 43 and 44 thus yield a lower and upper limit, respectively, and used together usually give a satisfactory estimate for the equilibrium time of a cascade.

Examination of equation 42 shows that T_{eq} is directly proportional to the average stage holdup of process material. Thus, in conjunction with the fact that liquid densities are on the order of a thousand times larger than gas densities at normal conditions, the reason for the widespread use of gas-phase processes in preference to liquid-phase processes in cascades for achieving difficult separations becomes clear.

The unsteady-state behavior of a separation unit is, furthermore, of interest because it can be used for the experimental determination of the separation parameters of the unit. If the holdup of the separating unit

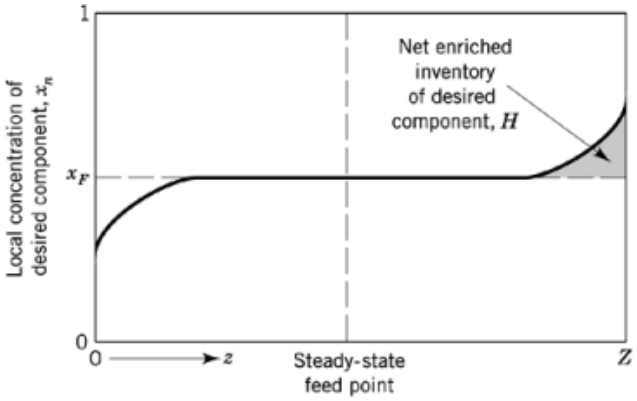

Fig. 6. Concentration gradient in a column or cascade a short time after start-up.

is known, the separation factor, $\alpha - 1$, can be obtained from a knowledge of the transient behavior of the unit during start-up. Figure 6 shows the concentration gradient in a square column shortly after start-up. As long as the gradient is flat at the feed point as shown, an equation much like equation 44 for the maximum equilibrium time can be used to relate the enriched holdup to the elapsed time. From a knowledge of the gradient, the enriched holdup H can be computed, and with L known the separation factor $\alpha - 1$ can be computed from

$$(\alpha - 1) = H/\left[Lx_F\,(1 - x_F)\,\Delta t\right] \qquad (45)$$

where Δt is the elapsed time since start-up when the column was filled with material at feed concentration.

3. The Gaseous Diffusion Process

The gaseous diffusion separation process depends on the separation effect arising from the phenomenon of molecular effusion (that is, the flow of gas through small orifices). When a mixture of two gases is confined in a vessel and is in thermal equilibrium with its surroundings, the molecules of the lighter gas strike the walls of the vessel more frequently, relative to its concentration, than the molecules of the heavier gas. This is caused by the greater average thermal velocity of the lighter molecules. If the walls of the container are porous with holes large enough to permit the escape of individual molecules, but sufficiently small so that bulk flow of the gas as a whole is prevented (that is, with pore diameters approaching mean-free-path dimensions of the gas), then the lighter molecules escape more readily than the heavier ones, and the escaping gas is enriched with respect to the lighter component of the mixture. The equation for the separation factor, α, for this process reflects the relative ease of light versus heavy molecules in escaping through the pores. Indeed, α^*, the ideal separation factor, is the ratio of the two molecular velocities. Because the kinetic energies, $1/2\ mv^2$, of the two species are the same, α^*, the ratio of the two velocities is equal also to the square root of the inverse ratio of the two molecular weights. In 1895 Rayleigh and Ramsey used this method to separate argon from nitrogen, and in 1920 it was employed to slightly enrich the concentration of the neon-22 isotope.

A primary improvement in diffusion separation technology was the development in 1932 of a cascade of diffusion stages for isotope separation by an arrangement similar to that shown in Figure 7. Using a 24-stage cascade an appreciable enrichment in the isotopes of neon was obtained. Subsequently (9), almost pure

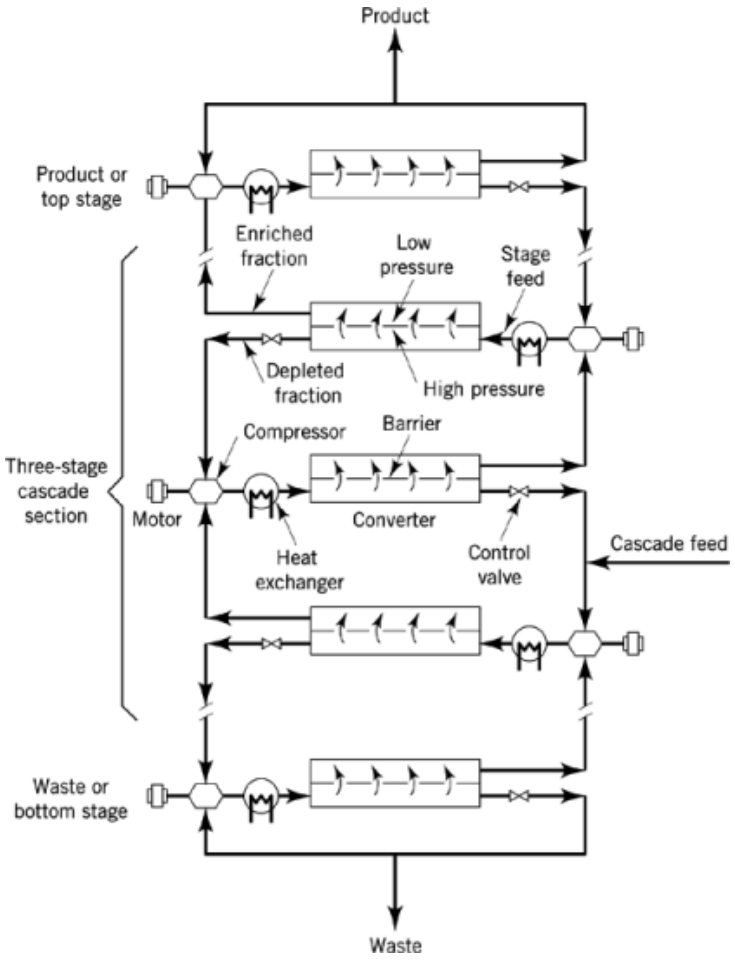

Fig. 7. A cascade of gaseous diffusion stages.

deuterium was obtained from a cascade of 48 stages, and the isotopes of nitrogen and of carbon were enriched (10) using a 34-stage cascade.

The large plants built for the separation of uranium isotopes following World War II are outstanding applications of the gaseous diffusion process. In the United States this work culminated in the construction of the gaseous diffusion cascade called the K-25 plant at Oak Ridge, Tennessee. Other plants were built at Oak Ridge, Paducah, Kentucky, and Portsmouth, Ohio, in the United States (11–13) and at Capenhurst, England (14), and at Pierrelatte and Tricastin, France (15). Gaseous diffusion plants have also been reported to be in operation in the former USSR and in the People's Republic of China.

3.1. Process Description

The basic unit of a gaseous diffusion cascade is the gaseous diffusion stage. The main components are the converter holding the barrier in tubular form, motors, and compressors moving the gas between stages, a heat exchanger removing the heat of compression introduced by the stage compressors, the interstage piping, and special instruments and controls to maintain the desired pressures and temperatures.

Figure 7 is a schematic representation of a section of a cascade. The feed stream to a stage consists of the depleted stream from the stage above and the enriched stream from the stage below. This mixture is first compressed and then cooled so that it enters the diffusion chamber at some predetermined optimum temperature and pressure. In the case of uranium isotope separation the process gas is uranium hexafluoride [7783-81-5], UF_6. Within the diffusion chamber the gas flows along a porous membrane or diffusion barrier. Approximately one-half of the gas passes through the barrier into a region of lower pressure. This gas is enriched in the component of lower molecular weight, ^{235}U. The enriched fraction, upon leaving the diffusion chamber, is directed to the stage above where it is recompressed to the barrier high-side pressure. The gas that does not pass through the barrier is depleted with respect to the light component. This depleted fraction, upon leaving the chamber, passes through a control valve, and is directed to the stage below where it too is recompressed to the barrier high-side pressure. However, because it is necessary in this case to compensate only for the frictional losses and the control valve pressure drop, the compression ratio may not need to be as high as that for the enriched fraction. Thus there is some freedom in the design of the stage; that is, two compressors might be used, a larger one for the enriched fraction and a smaller one for the depleted fraction; or the pressure drop across the control valve may be made equal to the pressure drop across the barrier so that both streams can be recompressed by the same compressor (this scheme, although wasteful of power, might make up for it in savings in equipment costs), or some other compromise mode of operation might be used.

For operational efficiency a number of gaseous diffusion stages are operated together in units referred to as cells and buildings. Cells and buildings. Cells and buildings can be removed from operation for routine maintenance and bypassed without disturbing the diffusion cascade.

Successful operation of the gaseous diffusion process requires a special, fine-pored diffusion barrier, mechanically reliable and chemically resistant to corrosive attack by the process gas. For an effective separating barrier, the diameter of the pores must approach the range of the mean free path of the gas molecules, and in order to keep the total barrier area required as small as possible, the number of pores per unit area must be large. Seals are needed on the compressors to prevent both the escape of process gas and the inflow of harmful impurities. Some of the problems of cascade operation are discussed in Reference 16.

The need for a large number of stages and for the special equipment makes gaseous diffusion an expensive process. The three United States gaseous diffusion plants represent a capital expenditure of close to 2.5×10^9 dollars (17). However, the gaseous diffusion process is one of the more economical processes yet devised for the separation of uranium isotopes on a large scale.

3.2. Stage Design

The important parameters of a separation cascade employing gaseous diffusion stages are the stage separation factor and the size of a stage required to handle the desired stage flows. Both of these parameters depend on the characteristics of the barrier.

3.2.1. Barrier Characteristics

The barrier material must be fine-pored and have many pores per unit area. Preparation and characterization of such a material presents a difficult technological problem. The characteristics of a barrier suitable for the separation of isotopes by gaseous diffusion are discussed in Reference 18, including various effective pore sizes and pore size distributions. Experimental techniques used to evaluate barrier characteristics are presented in Reference 19. These techniques include adsorption methods, electron microscopy, x-ray analysis, porosity measurements with mercury, permeability measurements with liquids and gases, and measurements of separation effectiveness. Barrier materials have pore sizes in the range of 10–30 nm (20). One electrolytic technique leads to a thin sheet material having about 10^{10} pores per square centimeter and radii on the order of 15 nm (21). The separating performance of a barrier has been evaluated by means of a 12-stage pilot plant (22).

3.2.2. Barrier Flow

An ideal separation barrier is one that permits flow only by effusion, as is the case when the diameter of the pores in the barrier is sufficiently small compared to the mean free path of the gas molecules. If the pores in the barrier are treated as a collection of straight circular capillaries, the rate of effusion through the barrier is governed by Knudsen's law (eq. 46):

$$N = \frac{4}{3}\,(2\pi MRT)^{-1/2}\,\frac{\phi d}{l}\,\left(p_f - p_b\right) \qquad (46)$$

where N is the molar flow of gas per unit area through the barrier, M is its molecular weight, R is the gas constant, T is the absolute temperature, φ is the fraction of the barrier area open to flow, d is the effective pore diameter, l is the pore length or thickness of the barrier, and p_{f} and p_{b} are the high- and low-side pressures of the barrier, respectively. In practice not all of the flow through the barrier is effusive flow. Through those pores where the diameters are of the order of the mean free path or greater, a nonseparative Poiseuille flow occurs. The two types of flow are additive and the total flow can be represented by

$$N = \frac{\alpha}{(M)^{1/2}}\,\left(p_f - p_b\right) + \frac{b}{\mu}\,\left(p_f^2 - p_b^2\right) \qquad (47)$$

where a and b are functions of temperature for a particular barrier and μ is the viscosity of the gas. The first term on the right is the contribution to the total flow of the effusive flow, the second that of the nonseparative Poiseuille flow. Because the pressure dependence of each type of flow is different, the constants a and b can be evaluated from a series of measurements at different pressures (24).

3.2.3. The Fundamental Separation Effect

An ideal-point separation factor can be defined on the basis of the separation obtained when a binary mixture flows through an ideal barrier into a region of zero back pressure. For this case an expression of the form of equation 46 can be written for each component. The flow of light component through the barrier is proportional to $p_{\mathrm{f}}x'/(M_{\mathrm{A}})^{1/2}$, and the flow of heavy component is proportional to $p_{\mathrm{f}}(1 - x')/(M_{\mathrm{B}})^{1/2}$ where x' is the mol fraction of the light component on the high-pressure side of the barrier and M_{A} and M_{B} are the mol wts of the light and heavy components, respectively. The concentration, y', of the effusing gas is therefore

$$y' = \frac{x'/(M_A)^{1/2}}{x'/(M_A)^{1/2} + (1 - x')/(M_B)^{1/2}} \qquad (48)$$

and from the definition of α (eq. 1), it follows that the ideal-point separation factor is equal to

$$\alpha^* = \frac{y'/(1 - y')}{x'/(1 - x')} = (M_B/M_A)^{1/2} \qquad (49)$$

which, for the case of uranium isotope separation using UF_6, is equal to 1.00429. As has been pointed out, this is also the expression for the ratio of the velocity of the light molecules to that of the heavy molecules.

3.2.4. The Stage Separation Factor

The stage separation factor, in all probability, is appreciably different from the ideal-point separation factor because of the existence of four efficiency terms:

- (*1*) A Barrier Efficiency Factor. In practice, diffusion plant barriers do not behave ideally; that is, a portion of the flow through the barrier is bulk or Poiseuille flow which is of a nonseparative nature. In addition, at finite pressure the Knudsen flow (25) is not separative to the ideal extent, that is, $(M_{\mathrm{A}}/M_{\mathrm{B}})^{1/2}$. Instead, the

degree of separation associated with the Knudsen flow is less separative by an amount that depends on the pressure of operation. To a first approximation, the barrier efficiency is equal to the Knudsen flow multiplied by a pressure-dependent term associated with its degree of separation, divided by the total flow.

- (*2*) A Back-Pressure Efficiency Factor. Because a gaseous diffusion stage operates with a low-side pressure p_b which is not negligible with respect to p_f, there is also some tendency for the lighter component to effuse preferentially back through the barrier. To a first approximation the back-pressure efficiency factor is equal to $(1 - r)$, where r is the pressure ratio p_b/p_f.
- (*3*) A Mixing Efficiency Factor. As the gas flows along the high-pressure side of the diffusion barrier, it becomes, as a result of the effusion process, preferentially depleted with respect to the lighter component in the neighborhood immediately adjacent to the barrier. As a result a concentration gradient perpendicular to the barrier is set up on the high-pressure side, and the average concentration x' of the light component in the bulk of the gas flowing past a point is greater than x'', the concentration of the light component at the surface of the barrier at that point. The mixing efficiency factor is equal to the ratio $(y' - x')/(y' - x'')$ as indicated in Figure 8. A value for the point mixing efficiency factor can be calculated from a consideration of diffusion through an effective film representing the resistance to diffusion. It is given by an expression of the form: $\exp(-Nl_f/\rho D)$, where l_f is the thickness of the effective film.
- (*4*) A Cut-Correction Factor. The stage separation factor has been defined as relating the concentrations in the streams leaving the stage. Because the concentrations, x' and y', on each side of the barrier are changing continuously as the gas flows through the diffusion stage, the relationship between the concentrations of the streams differs from the point relationship. This difference is taken into account with the cut correction factor. If the gas on the high-pressure side flows through the stage with no appreciable mixing taking place in the direction of flow, and if the effused fraction is withdrawn from the stage directly upon passing through the barrier, the cut correction can be calculated from material balance considerations. For this case, the exit or stream concentration of the stage upflow is equal to the average concentration of the effused gas, whereas the exit or stream concentration of the downflow is equal to the terminal concentration of the uneffused gas which is, of course, at maximum and not average depletion. Consequently, the stage separation factor relating to exit concentration is greater than the point separation factor, and the cut correction factor exceeds unity. (This phenomenon is analogous to cross-flow in a plate distillation column.)

The stage separation factor can therefore be related to the ideal-point separation factor by an equation of the form

$$(\alpha - 1) = (E_b)\ \left(E_p\right)\ (E_M)\ (E_c)\ \left(\alpha^* - 1\right) \qquad (50)$$

where

$$E_b = \text{barrier efficiency} = \frac{\text{separative flow through barrier}}{\text{total flow through barrier}} \qquad (51)$$

$$E_p = \text{back} - \text{pressure efficiency} = 1 - r \qquad (52)$$

$$E_M = \text{mixing efficiency} = \exp^{-Nlf/\rho D} \qquad (53)$$

and

$$E_c = \text{cut correction} = \frac{1}{\theta} \ln \frac{1}{1 - \theta} \qquad (54)$$

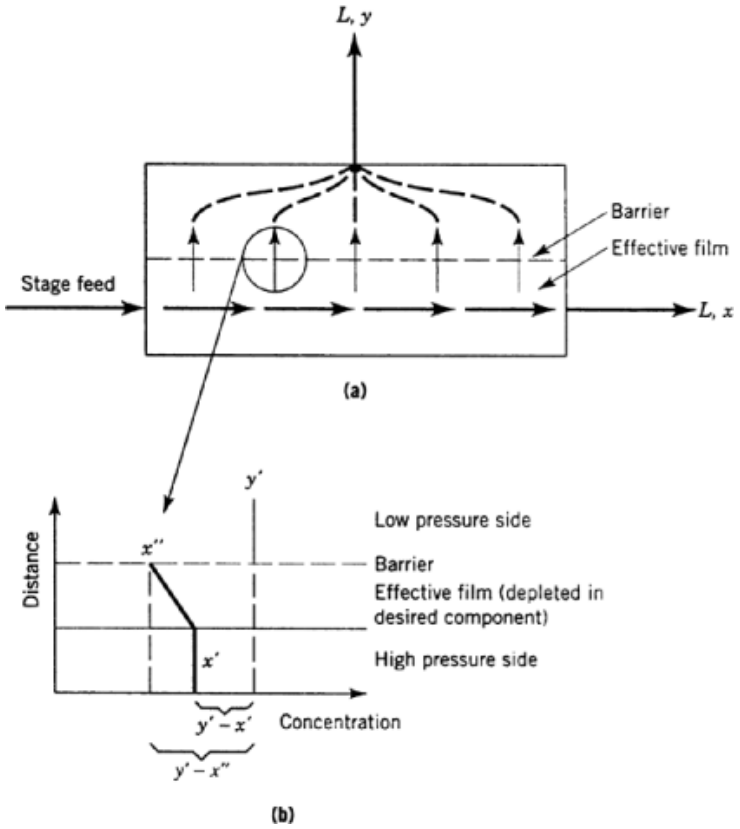

Fig. 8. Flow of process gas through a gaseous diffusion stage. (**a**) Gaseous diffusion stage; (**b**) local concentration profiles near the diffusion barrier; $_{y'=\text{point}}$ concentration of light component on low pressure side; $_{x'=\text{average}}$ concentration of light component in bulk of gas on high pressure side of barrier flowing past the specified point; $_{x''=\text{point}}$ concentration of light component at surface of barrier on the high pressure side; $_{y'-x''=\text{separation}}$ that would be obtained across barrier in the absence of the effective film; and $_{y'-x'=\text{actual}}$ separation obtained across barrier, taking a film into account.

For the usual case where approximately one-half of the gas entering the stage passes through the barrier, the value of the cut, θ, is equal to 0.5 and the cut correction takes on the value 1.386.

These efficiency factors are discussed in more detail in References (26–28). Actually, the barrier and backpressure efficiencies are interrelated and cannot be formulated independently, except only as an approximation. A better formation that has been found to fit the experimental results is:

$$(E_b)\ \left(E_p\right) = (1-r)\,/\left[1+(1-r)\ \left(p_f/p^*\right)\right] \qquad (55)$$

where p^* is a constant, the value of which must be determined experimentally. It may be noted that for an ideal barrier, $E_b = 1$, p^* is equal to ∞, and the backpressure efficiency is given by equation 52.

3.2.5. Separative Capacity

An expression for the separative capacity of a single gaseous diffusion stage where the upflow rate is L mols per unit time, given in equation 7, can be written as

$$\delta U = 1/4L\left(\frac{1-r}{1+(1-r)\ \left(p_f/p^*\right)}\right)^2 E_M^2\left(\frac{1}{\theta}\ln\frac{1}{1-\theta}\right)^2\ \left(\alpha^*-1\right)^2 \qquad (56)$$

For a very high quality barrier ($p^* \longrightarrow \infty$), the separative capacity of a stage having a mixing efficiency of 100% and operating at a cut of one-half would be:

$$\delta U = \frac{1.921}{4}\,L(1-r)^2\ \left(\alpha^*-1\right)^2 \qquad (57)$$

If the power requirement of the gaseous diffusion process were no greater than the power required to recompress the stage upflow from the pressure on the low-pressure side of the barrier to that on the high-pressure side, then the power requirement of the stage would be $LRT\ln(1/r)$ for the case where the compression is performed isothermally. The power requirement per unit of separative capacity would then be given simply by the ratio

$$\frac{\text{power requirement}}{\text{unit separative capacity}} = \frac{2.082\ RT}{\ln(1/r)}\,(1-r)^2\ \left(\alpha^*-1\right)^2 \qquad (58)$$

This quantity is minimized when the stage is operated at a pressure ratio across the barrier corresponding to $r = 0.285$. Furthermore, if power were the only economic consideration, the stage would be operated at this pressure ratio. However, as the value of r is decreased from this optimum, although the cost of power is increased, the number of stages required and hence the capital cost of the plant is decreased. Thus, in practice a compromise between these factors is made.

The optimum pressure level for gaseous diffusion operation is also determined by comparison; at some pressure level the decrease in equipment size and volume to be expected from increasing the pressure and density is outweighed by the losses that occur in the barrier efficiency. Nevertheless, because it is well known that the cost of power constitutes a large part of the total cost of operation of gaseous diffusion plants, it can perhaps be assumed that a practical value of r does not differ greatly from the above optimum. Inclusion of this value in the preceding equations yields

$$\delta U = 0.246\ L\left(\alpha^*-1\right)^2 \qquad (59)$$

and

$$\frac{\text{power requirement}}{\text{unit separative capacity}} = \frac{5.11\ RT}{(\alpha^*-1)^2} \qquad (60)$$

The actual power requirement is greater than that given by equation 58 or 60 because of the occurrence of frictional losses in the cascade piping, compressor inefficiencies, and losses in the power distribution system.

3.3. Plant Operation and Costs

The operation and economics of the three United States gaseous diffusion plants running in 1972 is discussed in References 29 and 30. These plants were operated as a single gaseous diffusion complex such that interplant shipments occurred so as to optimize the overall system. Independent operation of the plants would have resulted in about a 1% loss in separative work.

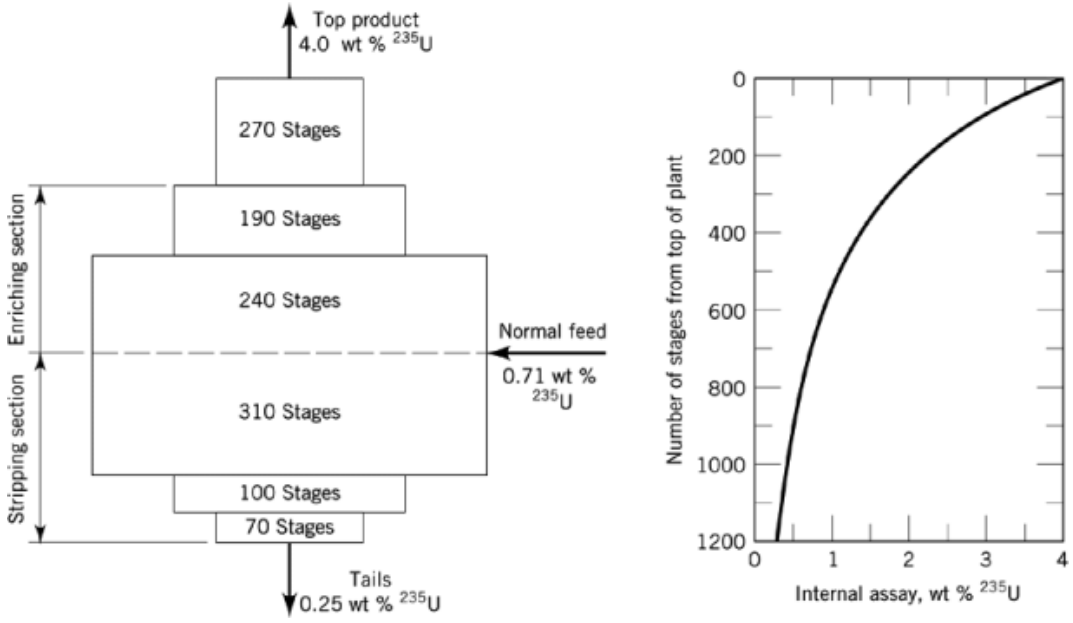

Fig. 9. Schematic diagram and internal gradient for an 8.75 million-SWU/yr plant.

In 1985, owing to the declining demand by the nuclear power industry for enriched uranium, the Oak Ridge gaseous diffusion plant was taken out of operation and, subsequently, was shut down. The U.S. gaseous diffusion plants at Portsmouth, Ohio and Paducah, Kentucky remain in operation and have a separative capacity of 19.6 million SWU (separative work unit) per year which as of this writing is not fully utilized.

Information on the design of new gaseous diffusion plants is available (30). The shape of a gaseous diffusion cascade, based on 1970 U.S. technology, having 8.75 million SWU/yr separative capacity, designed to produce uranium containing 4% ^{235}U from natural feed having tails at 0.25% ^{235}U is shown in Figure 9.

In 1973, Eurodif, a multinational consortium organized under French leadership, decided to build a large gaseous diffusion plant at Tricastin in France. This plant was completed in 1982, has a separative capacity of 10.8 million SWU/yr, and is based on French gaseous diffusion technology. Some design and progress information regarding this cascade is available (31–33). The engineering design of the French gaseous diffusion stage, although functionally the same as the United States stage, differs appreciably in appearance, and the motor, compressor, and diffuser are arranged vertically and are contained in a single housing in the French plant. Some of the main features of the Tricastin plant are UF_6 rates in kg/h of product, feed, and waste are 600, 3025, and 2425, respectively; percentage ^{235}U in the product, feed, and waste is 1.35–3.15, 0.72, and 0.25, respectively; stages in the enricher are 220 small sizes at 0.6 MW, 280 medium sizes at 1.6 MW, and 320 large sizes at 3.3 MW; stages in the stripper are 60 small sizes, 120 medium, and 400 large at 0.6, 1.6, and 3.3 MW, respectively; the total cascade power is 3100 MW, and the total cascade separative capacity is 10.7×10^6 SWU/yr; and the specific power requirement is 2538 kWh/SWU.

From equation 60 one can obtain a theoretical power requirement of about 900 kWh/SWU for uranium isotope separation assuming a reasonable operating temperature. A comparison of this number with the specific power requirements of the United States (2433 kWh/SWU) or Eurodif plants (2538 kWh/SWU) indicates that real gaseous diffusion plants have an efficiency of about 37%. This represents not only the barrier efficiency, the value of which has not been reported, but also electrical distribution losses, motor and compressor efficiencies, and frictional losses in the process gas flow.

The cost of enriched material from a gaseous diffusion plant depends both on the cost of separative work and of feed material. It can be seen from equation 15 that if the optimum tails concentration from a gaseous diffusion plant is 0.25%, the ratio of the cost of a kg of normal uranium to the cost of a kg of separative work equal to 0.80 is implied. Because the cost of separative work in new gaseous diffusion plants is expected to be about $100/SWU, equation 16 gives the cost per kg of uranium containing 4% ^{235}U as about $1,240.

4. Pressure Diffusion Processes

The development of the kinetic theory of gases led to the conclusion that a partial separation of the components of a gaseous mixture results when the gas is subjected to a pressure gradient. Thus, a column of gas standing in the earth's gravity field should show a separation effect, the lighter components concentrating at the top of the column, the heavier components at the bottom. This is indeed the case, but the effect is too slight to be utilized in a practical separation process. In the case of the isotopes of uranium, a column about 0.4 km in height would be required to give an enrichment equal to that of a single gaseous diffusion stage. Therefore, in order to utilize the pressure diffusion phenomenon, steeper pressure gradients than are normally available are needed.

Several devices have been developed for the purpose of producing such pressure gradients. The best known is the gas centrifuge (see also Separation, centrifugal). High-speed centrifuges can develop gravitational fields equal to many thousand times that of the earth. Thus relatively large pressure gradients can exist between the axis and periphery of a centrifuge, giving rise to appreciable separation effects. By moving streams of gas at the periphery and at the axis countercurrently, the centrifuge can be made equivalent to a multistage separating column.

A second type of apparatus based on the pressure diffusion effect is the separation nozzle. Pressure gradients in a curved expanding jet produce an isotopic separation similar to that in a centrifuge. The separation effect obtained with a single jet is relatively small, and separation nozzle stages, similar to gaseous diffusion stages, must be used in a cascade to realize most of the desired separations.

A third device that utilizes pressure diffusion is the vortex chamber. Here, as in the centrifuge, angular acceleration effects in a rapidly rotating gas provide the pressure gradient. The vortex chamber may be considered as a centrifuge with a stationary outer wall. The mechanical difficulties of high-speed rotating machinery are avoided at the expense of friction effects between the gas and the stationary wall. The literature concerning the use of such a device for isotope separation is limited. Results of experimentation indicate the effect of some of the process variables and the separation factors in H_2–CO_2, H_2–HD and ^{36}Ar–^{40}Ar binary gas mixtures have been measured (34, 35). A vortex tube has been used for isotope separation (36), and for the separation of gases in nuclear rocket or ramjet engines.

A vortex tubeprocess has been developed in South Africa and is being used there for the enrichment of uranium (37). It appears that cascades of this type are characterized by an extremely high power consumption.

4.1. The Gas Centrifuge

The first suggestion that centrifugal gravitational fields might be used to effect separation of isotopes was made in 1919 (38). Then in 1934 the convection-free vacuum ultracentrifuge was developed (39–41). Extensive information on the construction and operation of high-speed centrifuges and experimental data on the separation of the isotopes of argon, xenon, and uranium are available (39, 42–47). Early work on centrifuge development and centrifuge theory is discussed in References (48–55). Simplified approximate models of the flow have been developed (56–58), as have more accurate approximations (59–70). Japanese researchers have made an appreciable contribution to the literature in this field (71–78). Other surveys can be found in References 28 and (79–84). An excellent source of information on gas centrifuge development and centrifuge theory can be found

Table 1. Dimensions of Centrifuge Bowls[a]

Bowl	Length, cm	Radius, cm
UZ I	40	6.0
UZ IIIB	63.5	6.7
ZG 3	66.5	9.25
ZG 5	113.0	9.25
ZG 6[b]	240.0	20.0
ZG 7[b]	316.0	22.5
Zippe	30–38	3.81

[a] See Refs. 45 and 47.
[b] Proposed.

in the proceedings of the early workshops on gases in strong rotation and in the proceedings of the workshops on separation phenomena in gases and liquids which followed (85–91).

4.1.1. The Groth and Zippe Centrifuges

A schematic drawing of the ZG 5 gas centrifuge, in Figure 10, is typical of the Groth centrifuge (39, 45, 46). It is suspended and driven from above directly by an electric motor. The rotor spins in a vacuum-tight casing. Gas is introduced through a central tube and removed through scoop tubes at the ends of the rotor shielded by baffles from the main part of the bowl to prevent disturbance of the internal gas flow pattern. The gas is caused to undergo countercurrent axial flow by maintaining a temperature difference between the ends of the rotor. The top end of the bowl is heated by eddy currents in an aluminum ring at the top end cap; the bottom end cap is cooled by a cooling coil. Thermocouples are used to measure the end cap temperatures and the internal pressure at the centrifuge axis is measured by connections to the center tube. Labyrinth seals are used at the ends to maintain a gas seal.

The short bowl Zippe centrifuge (55) shown in Figure 11 is somewhat simpler. It is supported on a needle bearing at the base and driven by an electric motor, the armature of which is a steel plate rigidly attached to the bottom of the rotor. The stator consists of a flat winding on an iron core positioned so that the poles are separated from the armature by only a small gap (about 6 mm). Power is supplied by an alternator. Damping bearings are used to resist vibrations at both ends of the rotor. The centrifuge is completely closed at the bottom. The other end is connected with the top region of the outer vacuum casing only by a small annular gap around the feed tube. A small amount of gas that leaks from the interior of the bowl at the low pressure near the axis is confined to the region above the top of the rotor by a Holweck-type spiral groove molecular pump surrounding the rotor near the top, and pumped out of this region to maintain the necessary vacuum. Dimensions of the two types of centrifuges are given in Table 1.

The maximum theoretical separative capacity of a centrifuge is proportional to its length and to the fourth power of its peripheral speed, putting a premium particularly on high peripheral speeds and to a lesser extent on long rotors. The allowable peripheral speed of a cylindrical rotor is limited by the ratio of the tensile strength of the material of construction to its density. The maximum peripheral speed, or the burst speed, of a centrifuge rotor is given by:

$$V_{\max} = \left(\frac{\sigma}{\rho}\right)^{1/2} \qquad (61)$$

where σ is the tensile strength of the material and ρ is its density. The rotor must be resistant to the process gas, then only certain materials may be usable. Both Groth and Zippe centrifuges have used an aluminum alloy for rotors for use with UF_6. Table 2 gives the values of these properties for several materials that could be used for fabricating centrifuge rotors and the value of the corresponding maximum peripheral speed. The

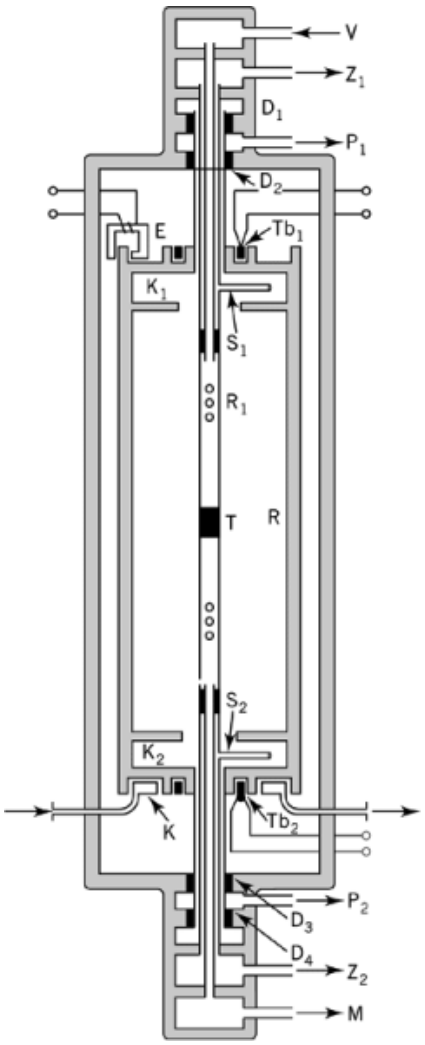

Fig. 10. The Groth ZG 5 centrifuge. R, rotor; R_1, stationary shaft; T, Teflon seal; K_1, K_2, chambers for gas scoops; S_1, S_2, scoops; V, gas supply; M, manometer; Z_1, Z_2, tapping points for enriched and depleted gas; P_1, P_2, vacuum chambers; E, electromagnet for eddy current heating; Tb_1, Tb_2, temperature measuring devices; K, cooling coil; and D_1, D_2, D_3, D_4, labyrinth seals.

allowable operating speed would be expected to be about 80% of the maximum speed in order to provide a margin of safety.

4.1.2. Mechanical Features

The construction and operation of a precision, highspeed centrifuge in a high vacuum environment presents some formidable mechanical problems. One difficulty with high-speed rotating machinery is the critical-speed phenomena. A long rod, or its equivalent, undergoes resonant vibrations at its fundamental and higher natural frequencies. This can cause large displacements from the axis of rotation unless the rod is properly restrained at high frequencies by damping devices capable of applying sufficient restraining forces. In the Zippe centrifuge

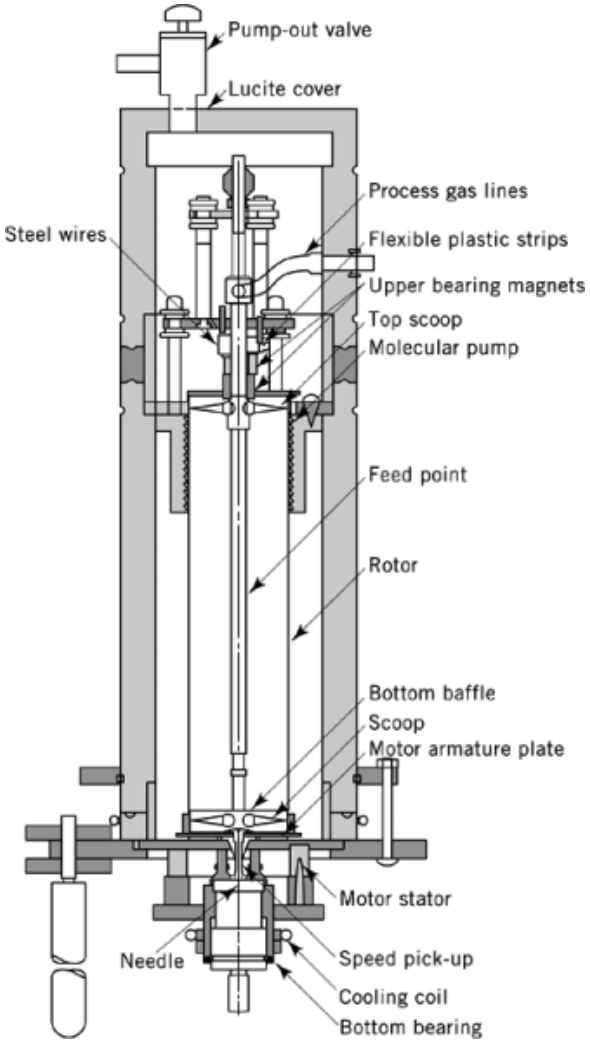

Fig. 11. The Zippe centrifuge.

the resonance frequency problem is avoided by limiting the ratio of length to diameter to less than four so that the customary operating speeds (300–350 m/s) are below the first fundamental flexural critical frequency, a so-called subcritical centrifuge. On the other hand Groth models, the ZG 6 and ZG 7, are long bowl or supercritical centrifuges. These run at rotational speeds above that corresponding to one or more flexural critical values and operate at a speed not too close to any of the critical values.

The principal power consumption of a centrifuge at operating speed occurs in friction in the bearing systems and in gas drag on the internal parts, particularly the scoops. A poorly balanced rotor results in high power consumption. Wide variations result from variations in the number, length, diameter of tubing, and tip design of the scoops (47). The long-term maintenance and lubrication of the bearing and support systems are a problem.

The scoop system in the Zippe centrifuge is used to control the internal circulation of the gas in the centrifuge, and in common with the Groth machines, must also extract a sufficient volume of gas at a pressure

Table 2. Maximum Peripheral Speeds for Various Rotor Materials

Material	Density, ρ, kg/m^3	Tensile strength, σ, GPa[a]	V_{max}, m/s
aluminum[b]	2800	0.448	400
aluminum[c]	2800	0.64	478
steel[b]	7800	1.381	421
maraging steel[b]	7800	1.932	498
maraging steel[c]	8100	3.0	608
glass fiber[b]	1800	0.49	522
carbon fiber[b]	1600	0.829	720
kevlar[c]	1334	2.17	1271
carbon fiber[c]	1560	3.50	1498

[a] To convert from GPa to psi, multiply by 145,000.
[b] From Ref. 82.
[c] From Ref. 90.

adequate to pump the gas to the feed point of the next centrifuge in a cascade. If this can be accomplished, no intermachine pumps are required in a cascade. This becomes an increasingly difficult problem at higher speeds because the scoop tips must be close to the centrifuge bowl wall in order to have access to the process gas at a higher pressure. The size and length of the piping in the scoops and the feed insertion tubing is critical because of limitations of their conductance for gas flow at low pressures. Other problems include long-term fatigue and creep of structural materials at high speeds and possibly stress corrosion in some systems. The Zippe centrifuge has been taken as the starting point for most of the modern centrifuge research and development programs.

The Urenco/Centec organization, formed in 1971 by British, Dutch, and German companies to carry on centrifuge research and development efforts, is a primary manufacturer and operator of centrifuge cascades for uranium enrichment. The research and development activities pursued by Urenco have succeeded roughly in doubling the separative capacity of individual centrifuges every five years since 1971. This has been accomplished primarily by increases in the length of the centrifuges and by increases in the peripheral speed of the centrifuges by the use of stronger and lighter materials of construction. Urenco currently operates commercial centrifuge enrichment facilities at Almelo in the Netherlands, at Capenhurst in England, and at Gronau in Germany. These plants have a combined separative capacity of 2.5 million SWU per year. A centrifuge plant to be built by Urenco having a separative capacity of 1.5 million SWU per year is planned for Homer, Louisiana.

An aggressive centrifuge development program culminating in the design, construction, and testing of large centrifuges that had a nominal separative capacity of 200 SWU per machine was carried out in the United States. This program was abandoned in 1985 before construction of the centrifuge facility in Portsmouth, Ohio, was completed. No gas centrifuge work has been done in the United States since that date. The former USSR has revealed that it has employed gas centrifuge technology for uranium enrichment since 1960 and that it operates centrifuge plants that have a combined separative capacity of 10 million SWU annually. Japan has also been developing gas centrifuges for a number of years. A 200,000 SWU uranium enrichment demonstration plant was placed in service at Ningyo-Toge in May 1989. A 1.5 million SWU/y gas centrifuge plant is under construction at Rokkashomura.

4.1.3. Design Principles

Although the separation of fluid mixtures can be accomplished using several different types of centrifuges, discussion of the centrifuge separation theory is herein confined to the consideration of the countercurrent gas centrifuge. In order to design separation cascades consisting of countercurrent gas centrifuges, it is necessary to know the separative performance of the individual units. Gas centrifuge theory serves fairly well for predicting the performance of a single centrifuge. However, the separation behavior of a particular gas centrifuge depends

on the flow pattern of the gas circulating within it, which in turn depends on the geometry of any baffles and scoops within the centrifuge bowl as well as on any temperature gradients in the gas and on the method used to introduce feed to the centrifuge. Owing to the complexity of the general case, the equations for centrifuge performance are presented for only a few idealized circulation patterns.

4.1.3.1. Radial Density and Pressure Gradients. Consider a centrifuge of length Z and of radius r_2, the internal dimensions of the centrifuge bowl, that rotates at a constant angular velocity of ω radians per second. If the centrifuge contains a single pure gas rotating at the same angular velocity as the centrifuge bowl, each element of the gas has a force impressed on it by virtue of its angular acceleration. This force is directed outward in a cylindrical coordinate system, and can be expressed as $(\rho\omega^2 r)(rdrd\varphi dz)$. At steady state this force must be balanced by a force resulting from the radial pressure gradient established in the centrifuge bowl. The inward force on an element of the gas owing to this pressure gradient is given by $(dp/dr)(rdrd\varphi\, dz)$. Equating these two forces gives:

$$dp/dr = \rho\omega^2 r \qquad (62)$$

where p is the pressure, r is the spatial coordinate in the radial direction, ρ is the density of the gas, and ω is the angular velocity of the centrifuge.

The pressure and the density of a gas are related by an equation of state. If the maximum pressure permitted within the centrifuge bowl is not too high, the equation of state for an ideal gas will suffice. The relationship between the pressure and density of an ideal gas is given by the well-known equation:

$$p = \rho RT/M \qquad (63)$$

where T is the absolute temperature of the gas, K; M is the mol wt of the gas, and R is the gas constant, 8.3147 J/(mol·K). Elimination of the density from equations 62 and 63 yields the differential equation for the pressure gradient in the centrifuge (eq. 64),

$$\frac{dp}{dr} = \frac{Mp}{RT}\omega^2 r \qquad (64)$$

which, for the case of an isothermal centrifuge, is readily integrated to yield

$$p(r) = p(0)\exp^{(M\omega^2 r^2/2RT)} \qquad (65)$$

Equation 65 gives the pressure at any point within the centrifuge, $p(r)$, as a function of the coordinate r, the pressure at the axis $p(0)$, the angular velocity of the centrifuge, and the temperature and mol wt of the gas. Should the centrifuge contain not a single pure gas, but a gas mixture, equations of the above forms could be written for each species present. In particular for the case of a binary gas mixture, consisting of species A and B.

$$p_A^{(r)} = p_A(0)\exp^{(M_A\omega^2 r^2/2RT)} \qquad (66)$$

and

$$p_B(r) = 2p_B(0)\exp^{(M_B\omega^2 r^2/2RT)} \qquad (67)$$

The ratio of these two equations gives the radial separation afforded by the gas centrifuge under equilibrium conditions, that is, for no internal gas circulation. An equilibrium separation factor between gas at the axis of

the centrifuge and gas at the periphery is therefore given by:

$$\alpha_0 \equiv \frac{x_A(0)}{x_B(0)} \Bigg/ \frac{x_A\left(r^2\right)}{x_B(r_2)} = \exp^{\left[(M_B - M_A)\omega^2 r_2^2/2RT\right]} \qquad (68)$$

It should be noted that the separation factor for the centrifuge process is a function of the difference in the mol wts of the components being separated rather than, as is the case in gaseous diffusion, a function of their ratio. The gas centrifuge process would therefore be expected to be relatively more suitable for the separation of heavy molecules. As an example of the equilibrium separation factor of a gas centrifuge, consider the Zippe centrifuge, operating at 60°C with a peripheral velocity ωr_2 of 350 m/s. From equation 68, α_0 is calculated to be 1.0686 for uranium isotopes in the form of UF_6.

4.1.4. Mass Transport

An expression for the diffusive transport of the light component of a binary gas mixture in the radial direction in the gas centrifuge can be obtained directly from the general diffusion equation and an expression for the radial pressure gradient in the centrifuge. For diffusion in a binary system in the absence of temperature gradients and external forces, the general diffusion equation retains only the pressure diffusion and ordinary diffusion effects and takes the form

$$J_A = -cD_{AB}\left[\frac{M_A x_A}{RT}\left(\frac{\bar{V}_A}{M_A} - \frac{1}{\rho}\right)\frac{dp}{dr} + \frac{dx_A}{dr}\right] \qquad (69)$$

where cD_{AB} is the product of the molar density and binary diffusion coefficient of the process gas and $\overline{V}_{\mathrm{A}}$ is the partial molal volume of component A.

Because the total pressure gradient is the sum of the partial pressure gradients, the following substitution can be made in equation 69

$$\frac{dp}{dr} = \frac{dp_A}{dr} + \frac{dp_B}{dr} = \frac{(M_A p_A + M_B p_B)}{RT}\omega^2 r \qquad (70)$$

and the equation for the radial flux of component A in a mixture of ideal gases is found to be

$$J_A = cD_{AB}\left[\frac{(M_B - M_A)\,x_A(1 - x_A)}{RT}\,\omega^2 r + \frac{dx_A}{dr}\right] \qquad (71)$$

Figure 12 is a schematic drawing of a section of a countercurrent gas centrifuge in which an arbitrary axial convective flow pattern is shown. It is assumed that the convective velocity v in the centrifuge can be expressed as a function of r only, and is independent of z. The convective velocity is assumed to be in the z direction only, and the regions at the ends of the centrifuge in which the direction of the flow is changed are neglected.

The net transport of component A in the $+z$ direction in the centrifuge τ_A is equal to the sum of the convective transport and the axial diffusive transport. At the steady state the net transport of component A toward the product withdrawal point must be equal to the rate at which component A is being withdrawn from the top of the centrifuge. Thus, the transport of component A is given by equation 72:

$$\tau_A = Px_P = \int_0^{r_2} 2\pi r c v x\,dr - \int_0^{r_2} 2\pi r c D_{AB}\frac{\partial x}{\partial z}\,dr \qquad (72)$$

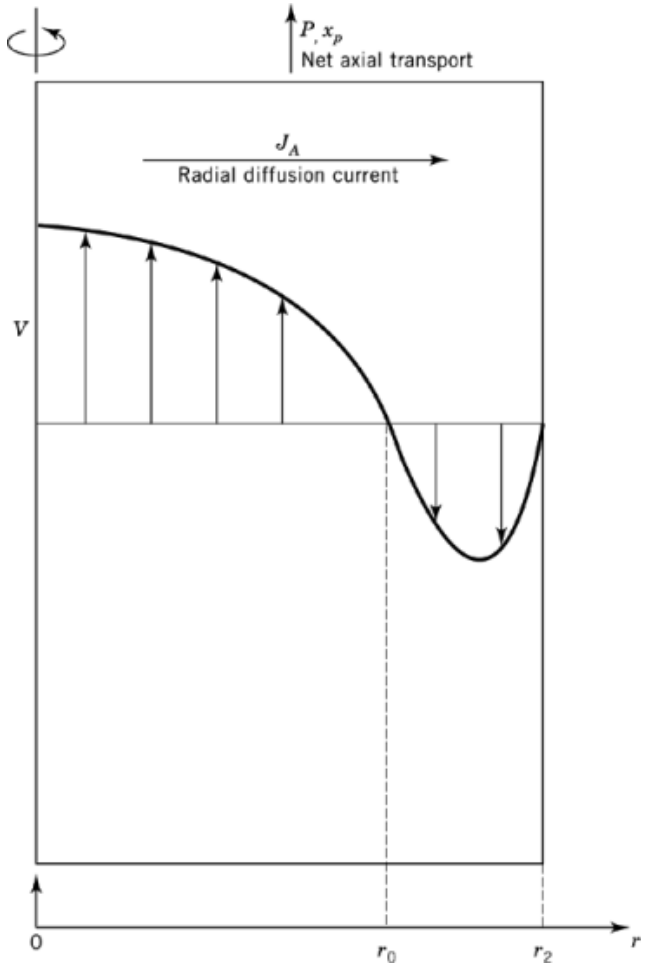

Fig. 12. Axial velocity profile in a countercurrent gas centrifuge.

where x is used in place of x_A for the mol fraction of component A, and the net transport of both components toward the product withdrawal point, τ, is given by

$$\tau = P = \int_0^{r_2} 2\pi r c v \, dr \qquad (73)$$

where P is the product withdrawal rate, mol/s, and x_P is the concentration of component A in the product material. The integrals appearing in equation 72 are evaluated using the flux equation 71 (92). Several approximations are involved and are most satisfactory for the case of relatively long units in which the axial concentration difference is large compared with the concentration differences in the radial direction, and in which the magnitudes of the feed and withdrawal rates are small with respect to the circulation rate of the internal convective flow. The results are not completely satisfactory for application to short-bowl centrifuges with relatively high throughput rates. For the case of the gas centrifuge, application of the method leads to a

gradient equation for the enriching section of the centrifuge that can be written in the form

$$S dx/dz = (\alpha - 1)\, x\,(1 - x) - (P/L)\ (x_P - x) \qquad (74)$$

where S is the stage length in the centrifuge and α is the stage separation factor. The quantity L is a measure of the convective circulation rate of the gas in the centrifuge and may be evaluated from the integral

$$L = \int_0^{r_0} 2\pi r c v\, dr \qquad (75)$$

where r_0 is the radius at which the convective velocity is equal to zero (see Fig. 12). The stage length S is the sum of two terms

$$S = \frac{\int_0^{r_2} \frac{dr}{rcD_{AB}} \left[\int_0^r r' c v\, dr'\right]^2}{\int_0^{r_0} rcv\, dr} + \frac{\int_0^{r_2} rcD_{AB}\, dr}{\int_0^{r_0} rcv\, dr} \qquad (76)$$

The first term may be considered as the contribution of the internal circulation or convective flow to the stage length, the second term as the contribution of the axial diffusion to the stage length. The stage separation factor is given by

$$\alpha - 1 = \frac{(M_B - M_A)\,\omega^2}{RT} \frac{\int_0^{r_2} r\, dr \int_0^r r' c v\, dr'}{\int_0^{r_0} rcv\, dr} \qquad (77)$$

From an inspection of the preceding three equations, it is evident that for the case of a given velocity profile in which v retains its functional dependence on r but is permitted to vary in magnitude by a factor, that is, $v = bf(r)$, the convective contribution to the stage length varies directly with the magnitude of L, whereas the diffusive contribution to the stage length varies inversely with the magnitude of the circulation rate L. Thus there exists a value of L for which the stage length for the separation process is a minimum. Designating this value of L by L_0, analysis of the expression for the stage lengths shows that

$$L_0 = 2\pi \int_0^{r_0} rcv\, dr \left[\frac{\int_0^{r_2} rcD_{AB}\, dr}{\int_0^{r_2} \frac{dr}{rcD_{AB}} \left(\int_0^r r' c v\, dr'\right)^2}\right]^{1/2} \qquad (78)$$

The corresponding minimum value of the stage length, designated by S_0, is given by

$$S_0 = \frac{2\left[\int_0^{r_2} \frac{dr}{rcD_{AB}} \left(\int_0^r r' c v\, dr'\right)^2 \int_0^{r_2} rcD_{AB}\, dr\right]^{1/2}}{\int_0^{r_0} rcv\, dr} \qquad (79)$$

The preceding two equations may be used to write the gradient equation for the countercurrent gas centrifuge in an alternative form. If the ratio of the actual gas circulation rate in the centrifuge to the circulation rate that minimizes the stage length L/L_0 is designated by m, then equation 74 may be rewritten

$$\left(\frac{1 + m^2}{2m}\right) S_0 \frac{dx}{dz} = (\alpha - 1)\, x\,(1 - x) - \frac{P}{mL_0}\ (x_P - x) \qquad (80)$$

For the stripping section of the centrifuge, that is, the section between the point at which the feed is introduced and the end at which the waste stream is withdrawn, the gradient equation has the corresponding form

$$\left(\frac{1+m^2}{2m}\right) S_0 \frac{dx}{dz} = (\alpha - 1)\, x\,(1-x) - \frac{W}{mL_0}\,(x - x_w) \qquad (81)$$

where W is the waste withdrawal rate, mol/s, and x_w is the concentration of component A in the waste material.

4.1.5. Maximum Separative Capacity and the Separative Efficiency

The separative efficiency of a gas centrifuge used for isotope separation is best defined in terms of separative work. Thus, the separative efficiency E is defined by

$$E = \frac{\delta U\,(\text{experimental})}{\delta U\,(\text{max})} \qquad (82)$$

where δU (experimental) is the actual separative work produced per unit time by the centrifuge under consideration and δU (max) is the maximum theoretical separative capacity of the machine. The maximum separative capacity of a gas centrifuge (41) is given by

$$\delta U\,(\text{max}) = \frac{\pi Z c D_{AB}}{2}\left(\frac{\Delta M V^2}{2RT}\right)^2 \qquad (83)$$

where δU is the separative capacity in mols per unit time, Z is the length of the rotor, ΔM is the difference in the mol wts of the components being separated, and V is the peripheral velocity of the centrifuge ($V = \omega r_2$). The expression for the maximum separative capacity of a centrifuge indicates a desirability for: (*1*) Low-temperature operation because the theoretical maximum separative capacity of a centrifuge varies inversely as the temperature; (*2*) Long centrifuge bowls because the theoretical maximum separative capacity varies directly as Z and that δU (max) is independent of the radius of the bowl; and (*3*) High peripheral velocity because the theoretical maximum separative capacity varies as the fourth power of the peripheral speed. At the higher speeds the predicted separative capacity increases with increasing peripheral speed much more slowly than the fourth-power relationship. Nevertheless, over the entire range of speeds investigated there is still an appreciable gain in separative capacity to be realized from an increase in speed.

4.1.6. Theoretical Formulation of the Separative Efficiency

The separative efficiency E of a countercurrent gas centrifuge may be considered to be the product of four factors, all but one of which can be evaluated on the basis of theoretical considerations. In this formulation the separative efficiency is defined by

$$E \equiv e_C e_I e_F e_E \qquad (84)$$

where e_C designates the circulation efficiency, e_I designates the ideality efficiency, e_F designates the flow pattern efficiency, and e_E designates the experimental efficiency and includes all phenomena such as turbulence and end effects not taken into account by the preceding terms. The circulation efficiency for a countercurrent gas centrifuge is given by

$$e_C = m^2/\left(1+m^2\right) \qquad (85)$$

As has been previously noted, m is the ratio of the rate at which gas flows upward in a centrifuge to the quantity L_0 that depends on the geometry of the bowl, the physical properties of the gas, and the flow pattern. Thus, m is directly proportional to the upflow rate. It is evident from the definition of e_C that it approaches unity as m takes on increasingly larger values. This is understood when it is realized that the circulation efficiency is representative of the loss in separative capacity owing to axial diffusion against the axial concentration gradient established in the bowl, and is, in fact, equal to the ratio of the convective contribution to the stage length of the sum of the convective and diffusive contributions, that is, to the total stage length. As m increases, the convective contribution of the stage length increases proportionally, and the diffusive contribution decreases as m^{-1}; at high circulation rates the diffusive transport becomes negligible with respect to the convective transport within the centrifuge.

The ideality efficiency takes into account the difference between the shape of a centrifuge that may be regarded as a square cascade and that of an ideal cascade. As has been pointed out in the section on cascade theory, the separative capacity of an element of length in a centrifuge is the greatest when the circulation rate L through the element bears a certain relationship to the withdrawal rate, withdrawal concentration, and the concentration in the centrifuge at that point, as has been indicated by equation 28. When this condition is satisfied the cascade is termed ideal. In a square cascade, however, this condition cannot be satisfied at more than a single point in the enricher and in the stripping sections. Thus, one can associate an efficiency with each point in the cascade that is a function of the departure of the actual flow from the ideal flow. The ideality efficiency may be regarded as the average of these point efficiencies over the entire cascade.

Analysis of the gradient equations for a countercurrent gas centrifuge shows that when the withdrawal rates are optimized, the ideal efficiency assumes a maximum value of 81%. Curves of the ideal efficiency for both a stripping and enriching section of five stages ($Z/S = 5$) are shown in Figure 13. The flow model assumed in these calculations is also shown. In order to achieve this maximum value of 0.81 for the ideality efficiency, it is necessary that in addition to operating at the optimum withdrawal rates there be no mixing of gas of unlike concentrations at the feed point. The difference in the behavior of the curves for the efficiency of the enriching and stripping sections results primarily from the fact that in the model considered the feed is assumed to enter the downflowing stream, and therefore the flows in the enriching and stripping sections are not symmetric.

The flow pattern efficiency e_F depends solely upon the shape of the velocity profile in the circulating gas. In terms of the integrals appearing in the gradient equation, the flow pattern efficiency is given by equation 86.

$$e_F = \frac{4\left(\int_0^{r_2} r\,dr \int_0^r r' c v\,dr'\right)^2}{c D_{AB} r_2^4 \int_0^{r_2} \frac{dr}{r c D_{AB}} \left(\int_0^r r' c v\,dr'\right)^2} \qquad (86)$$

To evaluate the flow pattern efficiency, a knowledge of the actual hydrodynamic behavior of the process gas circulating in the centrifuge is necessary. Primarily because of the lack of such knowledge, the flow pattern efficiency has been evaluated for a number of different assumed isothermal centrifuge velocity profiles.

4.1.7. The Optimum Velocity Profile

The optimum velocity profile (41), that is the velocity profile that yields the maximum value for the flow pattern efficiency, is one in which the mass velocity pv is constant over the radius of the centrifuge except for a discontinuity at the wall of the centrifuge ($r = r_2$). This optimum velocity profile is shown in Figure 14**a**. For this case the following values for the separation parameters of the centrifuge are obtained

$$\alpha - 1 = \frac{1}{2} \frac{\Delta M V^2}{2RT} \qquad (87)$$

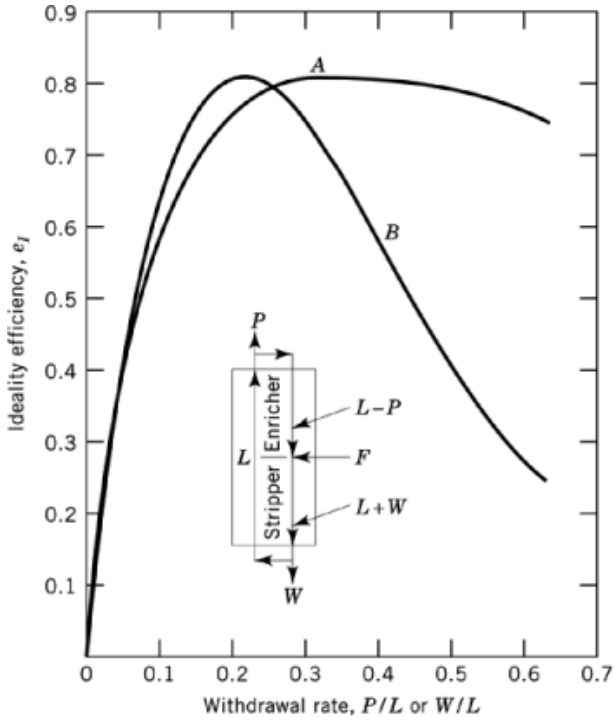

Fig. 13. The ideal efficiency of a five-stage enricher and stripper as a function of the product or waste withdrawal rate, where A represents stripping section efficiency, and B represents enriching section efficiency.

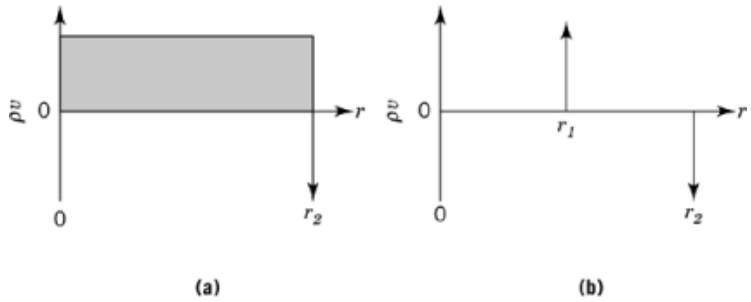

Fig. 14. Hypothetical velocity profile models for a countercurrent-flow gas centrifuge. (**a**) The optimum velocity profile in a countercurrent gas centrifuge. (**b**) The two-shell velocity profile.

$$L_0 = 2\,(2)^{1/2}\,\pi r_2 c D_{AB} \qquad (88)$$

$$S_0 = r_2\,(2)^{1/2} \qquad (89)$$

and $e_F = 1.0$.

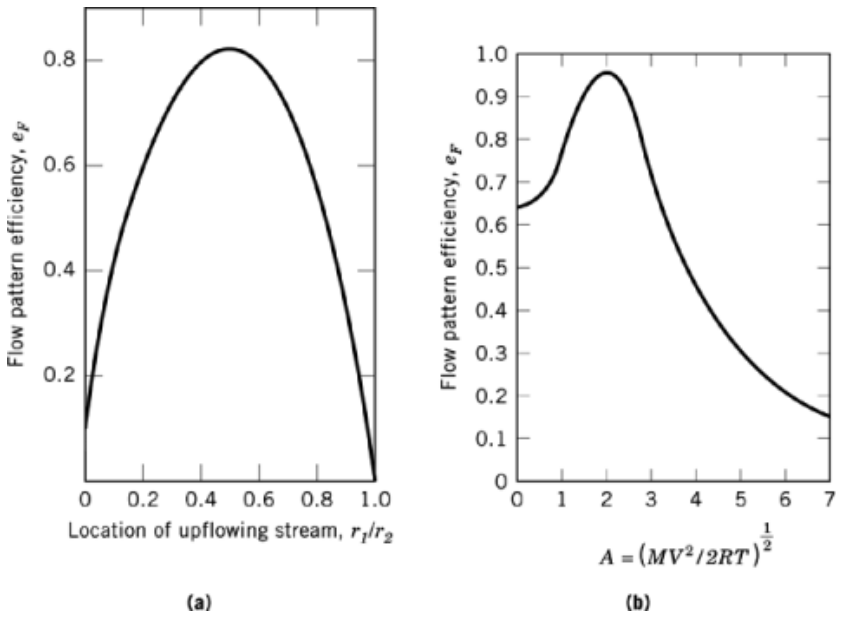

Fig. 15. (**a**) Values of the flow-pattern efficiency for the two-shell model. (**b**) The dependence of the flow-pattern efficiency on the dimensionless parameter A for the Martin profile.

4.1.8. The Two-Shell Velocity Profile

A second simple velocity profile (41) is shown in Figure 14**b** in which the flow consists of two thin streams, one situated at radius r_1, flowing upward, and the other situated at the wall ($r = r_2$), flowing downward. For this case the values of the separation parameters are

$$\alpha - 1 = \left[1 - \left(\frac{r}{1} r_2\right)^2\right] \frac{\Delta M V^2}{2RT} \qquad (90)$$

$$L_0 = \left[\frac{2}{\ln (r_2/r_1)}\right]^{1/2} \pi r_2 c D_{AB} \qquad (91)$$

$$S_0 = \left[2ln (r_2/r_1)\right]^{1/2} r_2 \qquad (92)$$

$$e_F = \left[1 - \left(\frac{r_1}{r_2}\right)^2\right]^2 \Big/ \ln \frac{r_2}{r_1} \qquad (93)$$

The value of the flow pattern efficiency is shown as a function of the spacing between the streams in Figure 15**a**. It can be seen that the flow pattern efficiency is a maximum when the position of the upflowing stream is chosen such that r_1/r_2 is equal to 0.5335. For this particular case the flow pattern efficiency assumes the value $e_F = 0.8145$.

These simple velocity profiles do not indicate directly any dependence of the flow pattern efficiency upon the rotational speed of the centrifuge. A dependence on speed is to be expected on the basis of the argument that at high speeds the gas in the centrifuge is crowded toward the periphery of the rotor and that the effective

distance between the countercurrent streams is thereby reduced. It can be seen from the two-shell model that, as the position of upflowing stream approaches the periphery, the flow pattern efficiency drops off from its maximum value.

4.1.9. The Martin Velocity Profile

It has been suggested (50) that the velocity profile in a gas centrifuge in which the countercurrent flow is caused by a temperature difference between the circulating gas and the end caps is given by

$$\int_0^r r' v \, dr' = \frac{\Delta T}{\omega} \left(\frac{\lambda^3}{\eta T} \right)^{1/4} \left(\frac{2rp(r_2)}{MRT} \right)^{1/2} \exp^{(M\omega^2(r^2 - r_2^2)/4RT)} \qquad (94)$$

where λ is the thermal conductivity of the process gas, η is the viscosity of the process gas, and ΔT is the temperature difference between the gas and the end caps, one warmer, the other cooler than the gas. Equation 94 was derived by considering the flow along a heated plate in a strong gravity field. All other considerations such as coriolis forces and any resistance to the axial flow, were neglected.

The separation parameters have been calculated for a centrifuge in which the behavior of the circulating gas is described by Martin's equation. The flow pattern efficiency is shown in Figure 15(**b**) as a function of the dimensionless parameter A, where A is equal to $(MV^2/2RT)^{1/2}$. In this case the maximum flow pattern efficiency attainable is 0.956.

4.1.10. Cascade Design

The efficiency of a Zippe-type centrifuge, separating uranium isotopes when UF_6 is the process gas, operating at a peripheral speed of 350 m/s and at a temperature of 320 K ($A = 2.85$), would be expected to be

$$E = \frac{m^2}{1 + m^2} \, (0.81) \, (0.76) \qquad (95)$$

The observed efficiency of 35% could be interpreted to mean that the circulation efficiency of this machine is about 60%, corresponding to an m value of 1.2. According to the theory presented, if the centrifuge could be operated with $m = 3$, it should be possible to obtain a separative efficiency of about 55%. With this assumption, the separative capacity of a single machine would be 1.78×10^{-3} kg/d of uranium. A cascade for uranium isotope separation designed to produce 1 kg/d of enriched uranium containing 90% ^{235}U from natural uranium would therefore require approximately 116,000 Zippe-type gas centrifuges. Table 3 shows the size of a cascade consisting of Zippe-type centrifuges required for the production of 1 kg/d of UF_6. Modern centrifuges have attained much higher separative capacities than the original Zippe machine. Were the cascade described in Table 3 to be constructed using today's centrifuges, the number of centrifuges required would be lower by one to two orders of magnitude.

5. The Separation Nozzle Process

The separation nozzle process, developed at the Karlsruhe Nuclear Research Center in Germany for the enrichment of the light uranium isotope ^{235}U, is also referred to as the jet diffusion method for the separation of gas mixtures. Isotopes were first separated (93) in a slit-type gas jet (94) in 1946. A device for separating gaseous mixtures by jet diffusion was patented in the United States in 1952. Soon thereafter this separation effect associated with high-speed gas flow through a nozzle was applied to the separation of isotopes (95–97). More recent work by the German research group is described (98–121). Interest in the jet separation process also led to experimental and theoretical work in the United States (94, 122–125), and in Japan (126–130).

Table 3. Characteristics of an Ideal Centrifuge Cascade[a]

Characteristics	Value	Source of value
Centrifuge parameters		
length of rotor Z, cm	30.48	given[b]
diameter of rotor $2r_2$, cm	7.62	given[b]
peripheral speed $V = wr_2$, m/s	350	given
operating temperature T, K	320	given
Centrifuge separative capacity		
separative capacity δU, SWU/yr, maximum	1.17	eq. 83
separative capacity, δU, SWU/yr, actual	0.65	E U(max)
circulation efficiency, e_c	0.90	eq. 85
ideality efficiency, e_I	0.81	maximum, Fig. 13
flow pattern efficiency, e_F	0.76	Fig. 15**b**, $A = 2.85$
Cascade parameters		
product concentration y_P, mol fraction	0.90	given
feed concentration X_F, mol fraction	0.0072	given
waste concentration x_W, mol fraction	0.0025	given
product rate P, kg/d	1.0	given
feed rate F, kg/d	191.0	eqs. 34, 35
separative capacity, δU, SWU/yr	75,380	eq. 36
number of centrifuges required	115,970	

[a] Cascade to yield 1 kg/d UF_6 enriched to 0.90 mol fraction ^{235}U.
[b] Predetermined by equipment or operation.

Table 4. Conceptual Design Data For a 5 Million SWU / yr Plant

Characteristics		Value	
separating element[a]			
N_0 (mol % UF_6)		4.2	
expansion ratio, π		2.1	
uranium cut, θ_u		1/4	
elementary separation effect E_A (%)		1.48	
separation nozzle inlet pressure, kPa[b]		38.7	
separation nozzle outlet pressure, kPa[b]		18.4	
separation stage	*Large*		*Small*
suction flow of compressor, m^3/h	1,030,600		312,000
rated power of compressor motor, kW	5,500		1,720
separating element slit length, m	26,660		8,050
separative work capacity, SWU/yr	12,800		3,900
cascade			
mass flow, kg/yr of U			
product[c]		1,585,000	
waste[d]		9,452,000	
feed[e]		11,037,000	
number of large stages		384	
number of small stages		186	
net separative work capacity, kg/yr of U		5,045,000	
total energy requirement of plant, MW		2,520	

[a] Hydrogen is used as a carrier gas.
[b] To convert kPa to mm Hg, multiply by 7.5.
[c] 3% ^{235}U.
[d] 0.337% ^{235}U.
[e] Natural uranium.

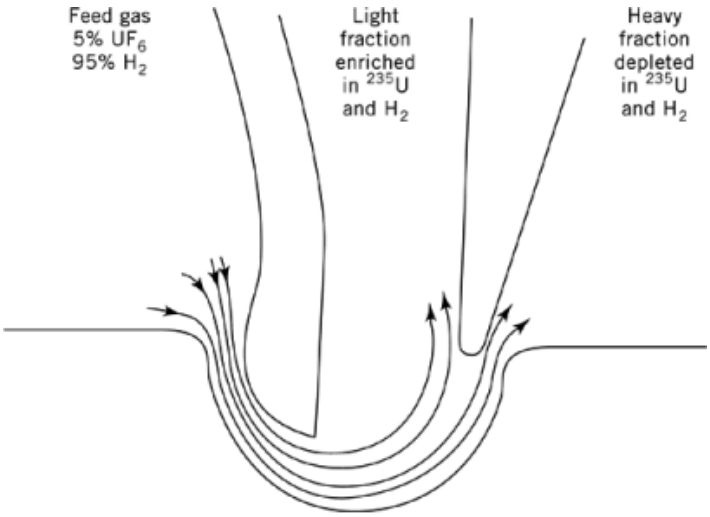

Fig. 16. Cross-section of the separation nozzle system used in the commercial implementation of the separation nozzle process.

5.1. Apparatus and Method of Operation

The separation nozzle process stage planned for commercial use differs appreciably from the stage used in early investigations. The basic features of the separation nozzle method are illustrated in Figure 16. Gaseous uranium hexafluoride mixed with a light auxiliary gas is expanded through a nozzle into a curved flow channel. At the end of the curved flow path, after turning 180°, the stream is divided by a knife edge into two parts, an interior fraction which is enriched in ^{235}U and a wall fraction which is depleted with respect to the ^{235}U. The light auxiliary gas present in a large molar excess increases the flow velocity of the UF_6 and, hence, it increases the centrifugal force determining the separation. In addition, the light gas delays the sedimentation of the two UF_6-isotopes in the centrifugal field slightly differently, which also has a favorable effect upon the separation of the isotopes.

Usually, a mixture of 2–5 mol % UF_6 and 95–98 mol % H_2 is used as a process gas; the expansion ratios range from 1.8–2.5. According to the gas kinetic scaling relations the optimum operating pressure of the nozzle is inversely proportional to its characteristic dimensions; for example, the optimum inlet pressure of a commercial separation nozzle system with a radius of curvature of 0.1 mm is on the order of tens of kPa (tenths of atmospheres). Figure 17 illustrates the design of a commercial separation nozzle element. The ten slit-shaped separation nozzles are mounted on the periphery of an extruded aluminum tube. Feed gas is introduced into the segments marked F and expands through the nozzles. The heavy fraction is pumped off through the segments marked H and the light fraction is pumped off from the space around the element.

5.2. Theory

A good understanding of the separation phenomenon of the separation nozzle process is obtained from a very simple model that treats the separation nozzle as a gas centrifuge at steady state. It is assumed that the feed mixture traverses the circular flow path at a constant and uniform angular velocity (wheel flow) and that the peripheral velocity of the flow is equal to the sonic velocity of the entering feed gas. The separation of the isotopes is effected, as in the gas centrifuge, by pressure diffusion in the pressure gradient resulting from the curved streamlines and the associated centrifugal forces. One important function served by the light auxiliary

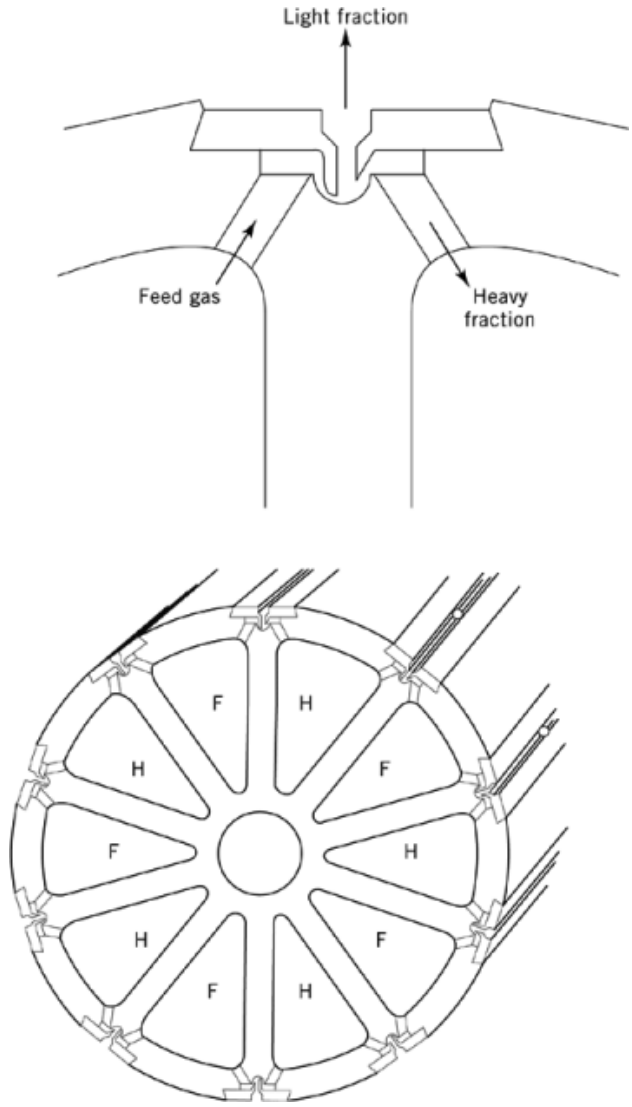

Fig. 17. Schematic representation of a commercial separation element tube manufactured by the Messerschmitt-Bölkow-Blohm Company, Munich. Terms are defined in text.

gas in the feed is to increase the flow velocity of the mixture and hence the magnitude of the separation factor attained.

When the gas speed is sufficiently high, the separation factor corresponding to a given value of the cut is essentially independent of the gas velocity and, hence, at high speeds, is given (104) to a good approximation as

$$(\alpha - 1)\left(\frac{1}{1-\theta}\ln\frac{1}{\theta}\right)\frac{\Delta M}{M} \qquad (96)$$

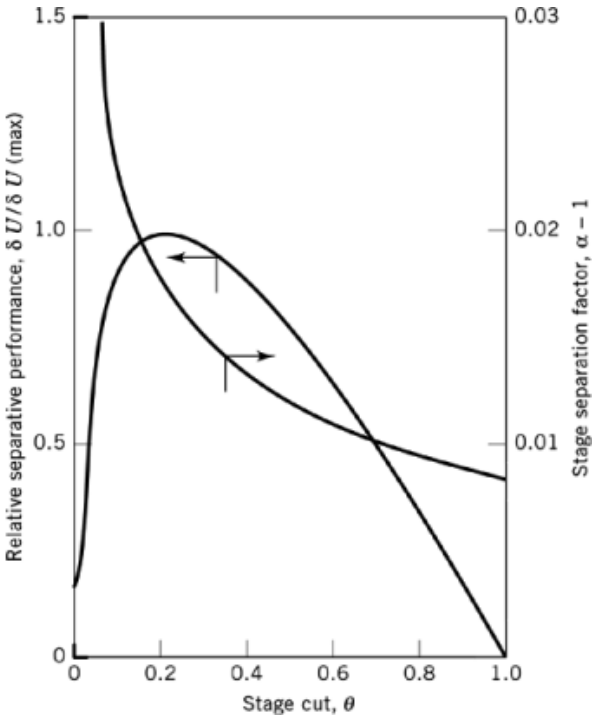

Fig. 18. High speed performance limit of an equilibrium separation nozzle.

where θ is the stage cut defined as the fraction of the uranium in the feed stream to the separation nozzle that is withdrawn in the light or enriched product stream and $\Delta M/M$ is the fractional difference in the mol wts of the isotopic species being separated. In the case of uranium isotopes where UF_6 is the process gas, $\Delta M/M = 3/352 = 0.0085$. The separative work produced by the stage is

$$\delta U = F\,\frac{\theta\,(1-\theta)}{2}\,(\alpha-1)^2 \qquad (97)$$

where F is the feed rate of uranium to the separating unit and δU is the amount of separative work produced by the nozzle system per unit time. The separation performance of the separation nozzle in the limit of high gas speed, as described in equations 96 and 97, is shown in graphical form in Figure 18. An equilibrium separation nozzle produces its maximum separative work rate at a cut of about 0.2. The secondary enrichment effects caused by ternary diffusion involving the light auxiliary gas, are treated in some detail in References 131 and 132.

5.3. Cascade for Uranium Enrichment

The design for a 5 million SWU/yr plant producing uranium enriched to 3% ^{235}U and stripping the feed to 0.3% ^{235}U in the waste stream is shown in Figure 19. Data for such a plant are given in Table 4. The 570 stages and 2520 MW required by the 5 million SWU/yr nozzle plant should be compared with the 1180 stages (to span the range from 0.25–4.0% ^{235}U) and 2430 MW required by the 8.75 million SWU/yr gaseous diffusion plant shown in Figure 9.

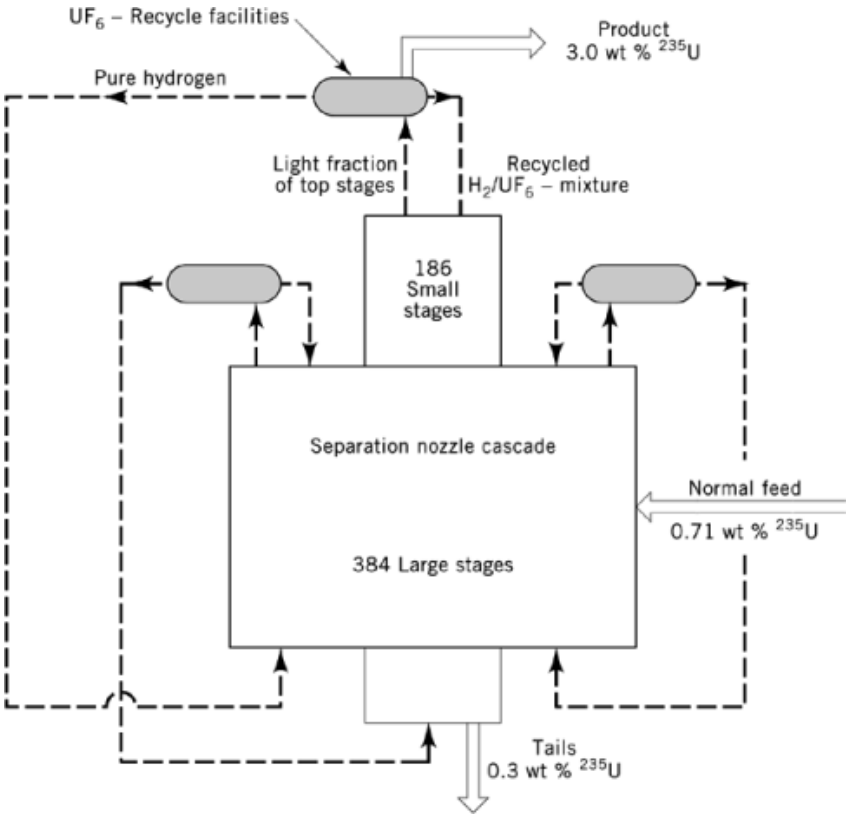

Fig. 19. Separation nozzle cascades of 5 million SWU/yr.

Three prototype separation nozzle stages of different sizes have been constructed at the Karlsruhe Nuclear Center. A small stage, designated the SR-33, has a compressor suction volume of 33,000 m^3/h, 7.5 m in height and 1.5 m in diameter. A stage of intermediate size, designated the SR-100, has a compressor suction volume of 100,000 cm^3/h, 10 m in height and 2.5 m in diameter. A large stage, designated the SR-300, has a compressor suction volume of 300,000 cm^3/h, 14 m in height and 4 m in diameter. When separation nozzle systems of an advanced design (double-deflecting nozzles having small radii of curvature of 20 μm and 10 μm) are installed in these stages, the separative capacity of the SR-33 stage is expected to be 2400 SWU annually; the separative capacity of the SR-100, 7200 SWU per year; and the separative capacity of the SR-300, 22,000 SWU per year. It was estimated in 1982 that a 3.8 million SWU per year cascade, designed to enrich uranium to 3.2 percent ^{235}U, would have a separative work cost of $120/SWU (75).

6. Nomenclature

C_{F}	= cost of feed material, eq. 14, \$/M or \$/mol.
$C_{\Delta U}$	= cost of separative work, eq. 14, \$/M or \$/mol.
C_{total}	= total cost of enriched product, eq. 14, \$/M or \$/mol.
c	= total molar concentration, mol/L^3.
D_{AB}	= binary diffusion coefficient for the pair A - B, L^2/t.
E	= overall efficiency of a separation process, eq. 82, dimensionless.
E_{b}	= barrier efficiency in gaseous diffusion, eq. 51, dimensionless.
E_{c}	= cut correction in gaseous diffusion, eq. 54, dimensionless.
E_{M}	= mixing efficiency in gaseous diffusion, eq. 53, dimensionless.
E_{p}	= back-pressure efficiency in gaseous diffusion, eq. 52, dimensionless.
e_{C}	= circulation efficiency of a centrifuge, eq. 85, dimensionless.
e_{E}	= experimental efficiency of a centrifuge, eq. 84, dimensionless.
e_{F}	= flow pattern efficiency of a centrifuge, eq. 86, dimensionless.
e_{i}	= ideality efficiency of a centrifuge, eq. 84, dimensionless.
F	= feed flow rate to a unit or cascade, eq. 34, M/t or mol/t.
H	= steady-state enriched inventory of desired component in a cascade, eq. 42, M or mols.
h_{n}	= total material holdup of the nth stage, eq. 42, m or mols.
J_4	= molar flux of component A in a binary mixture relative to the molar average velocity, eq. 69, mol/tL^2.
L	= upflow rate of process gas in a stage, eq. 3, M/t or mol/t.
L_{ideal}	= stage upflow of process gas in an ideal cascade, eq. 28, M/t or mol/t.
L_{min}	= minimum stage upflow of process gas, eq. 22, M/t or mol/t.
l_0	= value of interstage flow rate which minimizes the stage length, eq. 78. M/t or mol/t.
l_{f}	= thickness of effective stagnant film on gaseous diffusion barrier, eq. 53, L.
M_{i}	= molecular weight of component i.
m	= ratio of actual interstage flow rate to interstage flow rate which minimizes the stage length, eq. 80, dimensionless.
N_{A}	= molar flux of component A with respect to stationary coordinates, mol/L^2t.
N_{ideal}	= number of stages required to span a given concentration span in an ideal cascade, eq. 27, dimensionless
N_{min}	= minimum number of stages required to span a given range of concentrations, eq. 21, dimensionless.
N_{sect}	= number of stages required to span the concentration range of a square section, eq. 23, dimensionless.
n	= stage counting index, eq. 17, dimensionless.
P	= product flow rate of a unit or cascade, eq. 34, M/t or mol/t.
p	= fluid pressure, M/t^2L.
p_{b}	= fluid pressure on the low pressure side of the gaseous diffusion barrier, eq. 46, M/t^2L.
p_{f}	= fluid pressure on the high pressure side of the gaseous diffusion barrier, eq. 46, M/t^2L.
R	= gas constant, ML^2/t^2T mol.
r	= pressure ratio $p_{\mathrm{b}}/p_{\mathrm{f}}$ across the gaseous diffusion barrier, eq. 52,dimensionless.
r_0	= transverse coordinate of the plane of zero axial velocity, eq. 75, L.
r_2	= radius of a centrifuge bowl, eq. 68, L.
S	= stage length of a continuous process, L.
T	= absolute temperature, T.

T_{eq}	= equilibrium time of a cascade or separating unit, eq. 42, t.
δU	= separative capacity of a unit. eq. 3, M/t or mol/t.
ΔU	= separative capacity of a cascade, M/t or mol/t.
V	= peripheral velocity of a centrifuge, eq. 83, L/t.
$\overline{V}_A$	= partial molal volume of a component A in a mixture, eq. 69, L^3/mol.
$v(x)$	= value function, eq. 12, dimensionless.
$v'(x)$	= first derivative of the value function with respect to concentration, eq. 13, dimensionless.
$v''(x)$	= second derivative of the value function with respect to concentration, eq. 11, dimensionless.
W	= waste flow rate from a unit or cascade, eq. 34, M/t or mol/t.
x	= mol fraction of desired component of a binary mixture in the downflow or depleted stream, dimensionless.
x_F	= mol fraction of desired component of a binary mixture in the feed stream of a unit or cascade, dimensionless.
x_i	= mol fraction of component i in a mixture, dimensionless.
x_W	= mol fraction of desired component of a binary mixture in the waste stream of a unit or cascade, dimensionless.
y	= mol fraction of desired component of a binary mixture in the upflow or enriched stream, dimensionless.
y_P	= mol fraction of desired component of a binary mixture in the product stream of a unit or cascade, dimensionless.
Z	= overall length of the separating column, L.
z	= mol fraction of desired component of a binary mixture in the feed stream of a stage, eq. 4, dimensionless.
z	= axial distance or length coordinate in a column, L.
α	= stage separation factor, eq. 1, dimensionless.
α^*	= ideal stage separation factor, eq. 49, dimensionless.
α_0	= equilibrium stage separation factor in a centrifuge, eq. 90, dimensionless.
θ	= fraction of stage feed which goes into the stage upflow, "cut," eq. 3, dimensionless.
μ	= fluid viscosity, M/Lt.
ρ	= mass density, M/L^3.
$\overline{\tau}$;	= average net upward transport of desired material in a cascade approaching equilibrium, eq. 42, M/t or mol/t.
ω	= angular velocity, eq. 62, radians/t.

BIBLIOGRAPHY

"Diffusion Separation Methods" in *ECT* 1st ed., Vol. 5, pp. 76–133, by M. Benedict, Hydrocarbon Research, Inc.; "Diffusion Separation" in *ECT* 1st ed., 2nd Suppl., pp. 297–315, by K. B. McAfee, Jr., Bell Telephone Labs.; "Diffusion Separation Methods" in *ECT* 2nd ed., Vol. 7, pp. 91–175, by J. Shacter, E. Von Halle, and R. L. Hoglund, Union Carbide Corporation; in *ECT* 3rd ed., Vol. 7, pp. 639–723, by R. L. Hoglund, J. Shacter, and E. Von Halle, Union Carbide Nuclear Division.

Cited Publications

1. A. Kanagawa, I. Yamamoto, and Y. Mizuno, *J. Nucl. Sci. Tech.* **14**, 892 (1977).
2. G. Jansen and J. L. Robertson, *Analysis of Nonideal Asymmetric Cascades*, paper presented at American Chemical Society Meeting, Montreal, May 1976.
3. G. A. Garrett and J. Shacter, *Proceedings of the International Symposium on Isotope Separation*, Amsterdam, 1958, 17–31.

4. G. R. H. Geoghegan in Ref. 3, 518–523.
5. H. Barwich, *Ann. Physik* **20**, 70 (1957).
6. E. Oliveri, *Energia Nucl. Milan* **8**, 453 (1961).
7. J. C. Guais, *BNES Intern. Conference on Uranium Isotope Separation*, Paper 21, London, Mar. 5–7, 1975.
8. N. Ozaki and I. Harada, *BNES Intern. Conference on Uranium Isotope Separation*, Paper 22, London, Mar. 5–7, 1975.
9. H. Harmsen, G. Hertz, and W. Schütze, *Z. Physik* **90**, 703 (1934).
10. D. E. Wooldridge and W. R. Smythe, *Phys. Rev.* **50**, 233 (1936).
11. H. D. Smyth, *Atomic Energy for Military Purposes*, Princeton University Press, Princeton, N.J., 1945.
12. P. C. Keith, *Chem. Eng.* **53**, 112 (1946).
13. J. F. Hogerton, *Chem. Eng.* **52**, 98 (1945).
14. K. E. B. Jay, *Britain's Atomic Factories*, H. M. Stationery Office, London, 1954.
15. M. Molbert in J. R. Merriman and M. Benedict, eds., *Recent Developments in Uranium Enrichment, AIChE Symposium Series, No. 221*, Vol. **78**, *The Eurodif Program*, AIChE, New York, 1982.
16. H. Albert, *Proceedings of the U.N. International Conference on Peaceful Uses of Atomic Energy, 2nd Geneva*, Vol. **4**, P/1268, 1958, 412–417.
17. *Major Activities in the Atomic Energy Programs*, Jan.–Dec., 1962. U.S. Gov't. Printing Office, Washington, D.C., 1963.
18. D. Massignon in Ref. 16, P/1266, 388–394.
19. J. Charpin, P. Plurien, and S. Mommejac in Ref. 16, P/1265, 380–387.
20. C. Frejacques and co-workers in Ref. 16, P/1262, 418–421.
21. M. Martensson and co-workers in Ref. 16 P/181, 395–404.
22. O. Bilous and G. Counas in Ref. 16, P/1263, 405–411.
23. W. G. Pollard and R. D. Present, *Phys. Rev.* **73**, 762 (1948).
24. P. C. Carman, *Flow of Gases through Porous Media*, Butterworths Publications Ltd., London, 1956.
25. R. D. Present and A. J. de Bethune, *Phys. Rev.* **75**, 1050 (1949).
26. H. T. C. Pratt, *Countercurrent Separation Processes*, American Elsevier Publishing Company, Inc., New York, 1967.
27. C. Boorman in H. London, ed., *Separation of Isotopes*, George Newnes Ltd., London, 1961, Chapt. 8; D. Massignon, *Gaseous Diffusion*, in S. Villani, ed., *Topics in Applied Physics*, Vol. **35**, Springer-Verlag, New York, 1979.
28. M. Benedict, T. Pigford, and H. Levi, *Nuclear Chemical Engineering*, 2nd ed., McGraw-Hill Book Co., New York, 1981, Chapt. 14.
29. *AEC Gaseous Diffusion Plant Operations*, USAEC Report No. ORO-684, U.S. Atomic Energy Commission, Washington, D.C., Jan. 1972.
30. *AEC Data on New Gaseous Diffusion Plants*, USAEC Report No. ORO-685, U.S. Atomic Energy Commission, Washington, D.C., Apr. 1972.
31. *CEA Bulletin d'Informations Scientifiques et Techniques*, No. 206, 3-134, Sept. 1975 (in French).
32. G. Besse, *BNES International Conference on Uranium Isotope Separation*, Paper 17, London, Mar. 5–7, 1975.
33. J. P. Gougeau, *Developments in Uranium Enrichment, AIChE Symposium Series 169*, Vol. **73**, AIChE, New York, 1977, 12–14.
34. H. J. Mürtz and H. G. Nöller, *Z. Naturforsch.* **16a**, 569 (1961).
35. Ger. Pat. 1,154,793 (Sept. 26, 1963), H. G. Nöller.
36. K. Bornkessel and J. Pilot, *Z. Physik. Chem.* **221**, 177 (1962).
37. A. J. A. Roux, W. L. Grant, R. A. Barbour, R. S. Loubser, and J. J. Wannenburg, *Development and Progress of the South African Enrichment Project, International Conference of Nuclear Power and its Fuel Cycle*, IAEA-CN-36/300, Salzburg, Austria, May 1977.
38. F. A. Lindemann and F. W. Aston, *Phil. Mag.* **37**, 523 (1919).
39. W. Groth in H. London, ed., *Separation of Isotopes*, George Newnes Ltd., London, 1961, Chapt. 6.
40. J. W. Beams, L. B. Snoddy, and A. R. Kuhlthau in Ref. 16, P/723, 428–434.
41. K. Cohen, *The Theory of Isotope Separation as Applied to the Large-Scale Production of U-235*, Natl. Nuclear Energy Ser. Div. III, Vol. **1B**, McGraw-Hill Book Co., New York, 1951, Chapt. 6.
42. W. Groth, E. Nann, and K. H. Welge, *Z. Naturforsch.* **12a**, 81 (1957).
43. W. Groth and K. H. Welge, *Z. Physik. Chem.* **19**, 1 (1959).
44. W. Buland and co-workers, *Z. Physik. Chem. Frankfurt* **24**, 249 (1960).
45. W. E. Groth and co-workers in Ref. 16, P/1807, 439–446.

46. K. Beyerle and co-workers in Ref. 3, 667–694.
47. G. Zippe, *The Development of Short Bowl Ultracentrifuges*, Rept. EP-4420-101-60U, Research Laboratories for the Engineering Sciences, University of Virginia, Charlottesville, 1960.
48. A. Bramley, *Science* **92**, 427 (1940).
49. H. Martin and W. Kuhn, *Z. Physik. Chem.* **189**, 219 (1941).
50. H. Martin, *Z. Elektrochem.* **54**, 120 (1950).
51. M. Steenbeck, *Kernenergie* **1**, 921 (1958).
52. *Proceedings of the International Symposium on Isotope Separation*, Amsterdam, 1958, 695–700.
53. A. Kanagawa and Y. Oyama, *J. At. Energy Soc. Jpn.* **3**, 868 (1961).
54. A. Kanagawa and Y. Oyama, *Nippon Genshiryoku Gakkaishi* **3**, 918 (1961).
55. S. Whitley, *Revs. Modern Physics* **56**, 41 (1984).
56. A. S. Berman, *A Theory of Isotope Separation in a Long Countercurrent Gas Centrifuge*, Rept. K-1536, Union Carbide Corp., Nuclear Div., 1962.
57. A. S. Berman, *A Simplified Model for the Axial Flow in a Long Countercurrent Gas Centrifuge*, Rept. K-1535, Union Carbide Corp., Nuclear Div., 1963.
58. H. M. Parker and T. T. Mayo, IV, *Countercurrent Flow in a Semi-Infinite Gas Centrifuge*, Rept. UVA-279-63R, Research Laboratories for the Engineering Sciences, University of Virginia, Charlottesville, 1963.
59. J. L. Ging, *Countercurrent Flow in a Semi-Infinite Gas Centrifuge: Axially Symmetric Solution in the Limit of High Angular Speed*, Rept. EP-4422-198-62S, Research Laboratories for the Engineering Sciences, University of Virginia, Charlottesville, 1962.
60. J. L. Ging, *The Nonexistence of Pure Imaginary Eigenvalues and the Uniqueness Theorem for the Linearized Gas Flow Equations*, Rept. EP-4422-245-62S, Research Laboratories for the Engineering Sciences, University of Virginia, Charlottesville, 1962.
61. J. L. Ging, *Onsager Minimum Principle for Stationary Flow in Axially Symmetric Rotating Systems*, Rept. EP-3912-321-64U, Research Laboratories for the Engineering Sciences, University of Virginia, Charlottesville, 1964.
62. J. L. Ging, *Eigenvalue Problem—Limit of Low Angular Speed*, Rept. EP-3912-64U, Research Laboratories for the Engineering Sciences, University of Virginia, Charlottesville, 1964.
63. J. L. Ging, *Modified Minimum Principle for Stationary Flow in a Gas Centrifuge*, Rept. EP-3912-325-64U, Research Laboratories for the Engineering Sciences, University of Virginia, Charlottesville, 1964.
64. J. L. Ging, *Onsager Minimum Principle for Axially Decaying Eigenmodes*, Rept. EP-3912-326-64U, Research Laboratories for the Engineering Sciences, University of Virginia, Charlottesville, 1964.
65. G. F. Carrier and S. H. Maslen, *Flow Phenomena in Rapidly Rotating Systems*, Rept. TID 18065, U.S-D.O.E., 1962.
66. G. F. Carrier in H. Görtler, ed., *Proceedings of the Eleventh International Congress of Applied Mechanics*, Springer, Berlin, 1964.
67. Soubbaramayer in Ref. 27, Chapt. 4, Centrifugation.
68. H. G. Wood, *J. Fluid Mech.* **101**, 1 (1980).
69. R. J. Ribando, *A Finite Difference Solution of Onsager's Model for Flow in a Gas Centrifuge*, Rept. UVA-ER-822-83U, University of Virginia, Charlottesville, 1983.
70. J. J. H. Brouwers, *On the Motion of a Compressible Fluid in a Rotating Cylinder*, Doctoral Dissertation, The Technische Hogeschool, Twente, the Netherlands, June, 1976.
71. T. Sakurai and T. Matsuda, *J. Fluid Mech.* **62**, 727 (1974).
72. T. Sakurai, *J. Fluid Mech.* **72**, 321 (1975).
73. T. Matsuda, K. Hashimoto, and H. Takeda, *J. Fluid Mech.* **73**, 389 (1976).
74. K. Hashimoto, *J. Fluid Mech.* **76**, 289 (1976).
75. T. Matsuda and K. Hashimoto, *J. Fluid Mech.* **78**, 337 (1976).
76. T. Matsuda and K. Hashimoto, *J. Fluid Mech.* **85**, 433 (1978).
77. T. Kai, *J. Nucl. Sci. Technol.* **14**, 267 (1977).
78. T. Kai, *J. Nucl. Sci. Technol.* **14**, 506 (1977).
79. E. Von Halle, *The Countercurrent Gas Centrifuge for the Enrichment of U-235*, K/OA-4058, Union Carbide Nuclear Div., Oak Ridge, Tenn., Nov., 1977.
80. E. Krause and E. H. Hirschel, eds., *DFVLR—Colloquium*, Proz-Wahn, West Germany, 1970.
81. D. R. Olander, *Adv. Nucl. Sci. Technol.* **6**, 105 (1972).

82. D. G. Avery and E. Davies, *Uranium Enrichment by Gas Centrifuge*, Mills & Boon Ltd., London, 1973.
83. S. Villani, *Isotope Separation*, American Nuclear Society, 1976.
84. E. Rätz in E. Rätz *Aerodynamic Separation of Gases and Isotopes, Lecture Series 1978*, Von Karmen Institute for Fluid Dynamics, Belgium, 1978.
85. A. Soubbaramayer, ed., *Proceedings of the Second Workshop on Gases in Strong Rotation*, Cadarache, France, Apr. 1977.
86. G. B. Scuricini, ed., *Proceedings of the Third Workshop on Gases in Strong Rotation*, Rome, Mar. 1979.
87. E. Rätz, ed., *Proceedings of the Fourth Workshop on Gases in Strong Rotation*, Oxford, UK, Aug. 1981.
88. H. G. Wood, ed., *Proceedings of the Fifth Workshop on Gases in Strong Rotation*, Charlottesville, Va., June 1983.
89. Y. Takashima, ed., *Proceedings of the Sixth Workshop on Gases in Strong Rotation*, Tokyo, Aug. 1985.
90. K. G. Roesner and E. Rätz, eds., *Proceedings of the First Workshop on Separation Phenomena in Liquids and Gases*, Technische Hochschule Darmstadt, Darmstadt, Germany, July 1987.
91. P. Louvet, P. Noe, and Soubbaramayer, eds., *Proceedings of the Second Workshop on Separation Phenomena in Liquids and Gases*, Cite Scientifique Parcs et Technopoles Ile de France Sud, Versailles, France, July 1989.
92. W. H. Furry, R. C. Jones, and L. Onsager, *Phys. Rev.* **55**, 1083 (1939).
93. P. A. Tahourdin, *Final Report on the Jet Separation Methods*, Oxford Rept. No. 36, Br. 694, Clarendon Lab., Oxford, UK, 1946.
94. S. A. Stern, P. C. Waterman, and T. F. Sinclair, *J. Chem. Phys.* **33**, 805 (1960).
95. E. W. Becker and co-workers in Ref. 16, P/1002, 455–457.
96. E. W. Becker in Ref. 3, 560–578.
97. E. W. Becker in H. London, ed., *Separation of Isotopes*, George Newnes Ltd., London, 1961, Chapt. 9.
98. E. W. Becker and co-workers, *Angew. Chemie. Intern. Ed. (Engl.)* **6**, 507 (1967).
99. E. W. Becker and co-workers, *Atomwirtschaft* **18**, 524 (1973).
100. E. W. Becker and co-workers, *International Conference on Uranium Isotope Separation*, London, 1975.
101. E. W. Becker and co-workers, *European Nuclear Conference*, Paris, 1975.
102. E. W. Becker and co-workers, American Nuclear Society Meeting, *KFK-Bericht 2235*, Gesellschaft für Kernforschung, Karlsruhe, 1975.
103. H. Geppert and co-workers, *International Conference on Uranium Isotope Separation*, London, 1975.
104. E. W. Becker and co-workers, *Z. Naturforsch.* **26a**, 1377 (1971).
105. P. Bley and co-workers, *Z. Naturforsch.* **28a**, 1273 (1973).
106. K. Bier and co-workers, *KFK-Bericht 1440*, Gesellschaft für Kernforschung, Karlsruhe, 1971.
107. U. Ehrfeld and W. Ehrfeld, *KFK-Bericht 1634*, Gesellschaft für Kernforschung, Karlsruhe, 1972.
108. W. Ehrfeld and E. Schmid, *KFK-Bericht 2004*, Gesellschaft für Kernforschung, Karlsruhe, 1974.
109. Ger. Pat. 1,096,875 (Jan. 12, 1961), E. W. Becker (to Deutsche Gold-und Silber-Scheideanstalt vorm. Roessler).
110. W. Ehrfeld and U. Knapp, *KFK-Bericht 2138*, Gesellschaft für Kernforschung, Karlsruhe, 1975.
111. E. W. Becker and co-workers, *4th United Nations International Conference on the Peaceful Uses of Atomic Energy*, Geneva, 1971, paper 383.
112. H. J. Fritsch and R. Schütte, *KFK-Bericht 1437*, Gesellschaft für Kernforschung, Karlsruhe, 1971.
113. R. Schütte and co-workers, *Chemie-Ing. Technik* **44**, 1099 (1972).
114. W. Fritz and co-workers, *Chemie-Ing. Technik* **45**, 590 (1973).
115. R. Schütte, *KFK-Bericht 1986*, Gesellschaft für Kernforschung, Karlsruhe, 1974.
116. P. Bley and co-workers, *KFK-Bericht 2092*, Gesellschaft für Kernforschung, Karlsruhe, 1975.
117. W. Ehrfeld in Ref. 84.
118. U. Ehrfeld in Ref. 84.
119. E. W. Becker in Ref. 27.
120. E. W. Becker, P. Noguira Batista, and H. Volcker, *Nucl. Technol.* **52**, 105 (1981).
121. E. W. Becker and co-workers in Ref. 16.
122. P. C. Waterman and S. A. Stern, *J. Chem. Phys.* **31**, 405 (1959).
123. R. R. Chow, *On the Separation Phenomenon of Binary Gas Mixture in an Axisymmetric Jet*, Rept. HE-150-175, Institute of Engineering Research, University of California, Berkeley, 1959.
124. E. E. Gose, *Am. Inst. Chem. Engs. J.* **6**, 168 (1960).
125. V. H. Reis and J. B. Fenn, *J. Chem. Phys.* **39**, 3240 (1963).

126. H. Mikami, *J. Nucl. Sci. Technol.* **6**, 452 (1969).
127. H. Mikami, *I & EC Fundam.* **9**, 121 (1970).
128. H. Mikami and Y. Takashima, *Bull. Tokyo Inst. Technol.* **61**, 67 (1964).
129. H. Mikami and Y. Takashima, *J. Nucl. Sci. Technol.* **5**, 572 (1968).
130. H. Mikami and Y. Takashima, *Int. J. Heat Mass Transfer* **11**, 1597 (1968).
131. W. Berkahn, W. Ehrfeld, and G. Krieg, *Calculations of Uranium Isotope Separation in the Separation Nozzle for Small Mol Fractions of UF_6 in the Auxiliary Gas*, Institut für Kernverfahrenstechnik, Kernforschungszentrum Karlsruhe, West Germany, report KFK-2351, Nov., 1976.
132. G. F. Malling and E. Von Halle, *Aerodynamic Isotope Separation Processes for Uranium Enrichment: Process Requirement*, paper presented at the Symposium on New Advances in Isotope Separation, Div. of Nuclear Chemistry and Technology, American Chemical Society, San Francisco, Calif., Aug. 1976; *UCC-ND Report K/OA-2872*, Oak Ridge Gaseous Diffusion Plant, Oak Ridge, Tenn., Oct. 7, 1976.

General References

133. M. Benedict, T. Pigford, and H. Levi, *Nuclear Chemical Engineering*, 2nd ed., McGraw-Hill Book Co., New York, 1981, Chapts. 12 and 14.
134. K. P. Cohen, *The Theory of Isotope Separation as Applied to the Large-Scale Production of U-235, National Nuclear Energy Series Division III*, Vol. **1B**, McGraw-Hill Book Co., New York, 1951.
135. H. London, ed., *Separation of Isotopes*, George Newnes Ltd., London, 1961.
136. H. R. C. Pratt, *Countercurrent Separation Processes*, American Elsevier Publishing Company, Inc., New York, 1967.
137. S. Villani, *Isotope Separation*, American Nuclear Society Monograph, ANS Publications, 1976.
138. S. Villani, ed., *Topics in Applied Physics*, Vol. **35**, Springer-Verlag, New York, 1979.
139. J. Kistemaker, J. Bigeleisen, and A. O. Neir, eds., *Proceedings of the International Symposium on Isotope Separation*, Amsterdam, Apr. 23–27, 1957, North-Holland Publishing Company, Amsterdam, and Interscience Publishers, Inc., New York, 1958.
140. *Proceedings of the Second United Nations International Conference on the Peaceful Uses of Atomic Energy*, Geneva, Sept. 1–3, 1958, United Nations publication, Geneva, 1958, particularly Vol. 4: *Production of Nuclear Materials and Isotopes*.
141. *Proceedings of the Third International Conference on the Peaceful Uses of Atomic Energy*, Geneva, Aug. 31–Sept. 9, 1964, United Nations publication, New York, 1965, particularly Vol. 12: *Nuclear Fuels—III, Raw Materials*.
142. *Proceedings of the Fourth International Conference on the Peaceful Uses of Atomic Energy*, Geneva, Sept. 6–16, 1971, United Nations and the International Atomic Energy Agency, 1972, particularly Vol. 9, *Isotope Enrichment, Fuel Cycles and Safeguards*.
143. *Proceedings of the International Conference on Uranium Isotope Separation*, London, Mar. 5–7, 1975, British Nuclear Energy Society, 1975.
144. M. Benedict, ed., *Development in Uranium Enrichment, AIChE Symposium Series*, Vol. **73**, No. 169, American Institute of Chemical Engineers, New York, 1977.
145. J. R. Merriman and M. Benedict, eds., *Recent Developments in Uranium Enrichment, AIChE Symposium Series*, Vol. **78**, no. 221, American Institute of Chemical Engineers, New York, 1982.

E. VON HALLE
Martin Marietta Energy Systems
J. SHACTER
Consultant

Related Articles

Separation systems, synthesis; Adsorption; Membrane technology